UNIVERSITY OF CALIFORNIA

Los Angeles

Epigenome and the lipidome rewiring for targeting IDH-mutant-gliomas

A dissertation submitted in partial satisfaction of

the requirements for the degree Doctor of Philosophy

in molecular biology

by

Lubayna Elahi

2023

ABSTRACT OF DISSERTATION

Epigenome and the lipidome rewiring for targeting IDH-mutant-gliomas

by

Lubayna Elahi

Doctor of Philosophy in Molecular Biology

University of California, Los Angeles, 2023

Professor Harley I. Kornblum, Chair

Missense mutation in the gene isocitrate dehydrogenase (IDH) rewires the metabolic and chromatin landscape of IDH mutant (MT) gliomas making them distinct from IDH wildtype (WT) gliomas. There is an intimate relationship between the epigenome and lipidome. In this study, we discovered valproic acid (VPA) a broad-spectrum anti-epileptic and histone deacetylase (HDAC) inhibitor modifies both the chromatin and the lipidome of IDH MT gliomas. We find that VPA significantly upregulates transcription of genes, but this does not necessarily correlate with increased overall chromatin accessibility. We identified a subset of lipogenic enzymes that are all downregulated with VPA treatment and show loss of chromatin accessibility around their promoter region. We characterized inhibition of one those enzymes FASN and show that both VPA treatment and FASN inhibition remodels the lipidome of IDH MT glioma and this remodeling is

distinct from what we see in a IDH WT cell line. Lastly, due to metabolic flexibility of IDH MT glioma cells we propose combination of VPA with a FASN inhibitor might be a better way of targeting IDH MT gliomas.

The dissertation of Lubayna Elahi is approved.

Albert Lai

Frank Pajonk

David Nathanson

William Lowry

Harley I Kornblum, Committee chair

University of California, Los Angeles

2023

Table of Contents

List of Figures

Chapter 1

Chapter 2

Chapter4

List of Tables

Acknowledgement

First and foremost, I would like to thank God Almighty for giving me patience and guidance and the ability to think and write this PhD dissertation.

Second, I would like to thank my family, especially my parents and my husband. Without their sacrifice and support I wouldn't be here at UCLA writing my PhD thesis.

Third, I would like to thank Dr. Harley Kornblum who graciously accepted me as a graduate student and mentored me for the last 5 years. Without Harley I would not have a dissertation lab.

Fourth, I would like to thank my committee members for their valuable guidance during committee meetings.

Lastly, I would like to thank all my lab mates, collaborators, and friends here at UCLA. Without them this journey would be much more difficult.

Biographical Sketch

Lubayna S Elahi

Education

2017-2023 University of California, Los Angeles, Los Angeles, CA

PhD Candidate, Department of Molecular Biology

2014-2017 San Jose State University, San Jose, CA

M.S. Physiology

2009-2013 San Jose State University, San Jose, CA

B.S. Physiology

Academic and Professional Honor

TCCI Writing Fellowship 2022

CIRM Scholar, 2015

F. Albert and Dorothy Ellis Research Fellowship, 2015

Claudia Greathead Research Fellowship, 2015

Selected Peer Review Publication

Elahi, L. S., Shamai, K. N., Abtahie, A. M., Cai, A. M., Padmanabhan, S., Bremer, M., & Wilkinson, K. A. (2018). Diet induced obesity alters muscle spindle afferent function in adult mice. *PLoS ONE*, *13*(5). https://doi.org/10.1371/journal.pone.0196832

Yoon, S.-J., Elahi, **L. S.**, Pașca, A. M., Marton, R. M., Gordon, A., Revah, O., Miura, Y., Walczak, E. M., Holdgate, G. M., Fan, H. C., Huguenard, J. R., Geschwind, D. H., & Pașca, S. P. (2019). Reliability of human cortical organoid generation. *Nature Methods*, *16*(1), 75–78. https://doi.org/10.1038/s41592-018-0255-0

Garrett, M. C., Albano, R., **Elahi, L**., Behrman, C., Pemberton, M., Woo, D., O'brien, E., Vancauwenbergh, B., Perentesis, J., Shah, S., Hagan, M., Zhao, C., Plas, D., Paranjpe, A., Roskin, K., & Lu, R. (2022). *HDAC1 and HDAC6 are essential for driving growth in IDH1 mutant glioma*. https://doi.org/10.21203/rs.3.rs-1720726/v1 (In Press)

Watanabe, M., Buth, J. E., Haney, J. R., Vishlaghi, N., Turcios, F., **Elahi, L**. **S**., Gu, W., Pearson, C. A., Kurdian, A., Baliaouri, N. V., Collier, A. J., Miranda, O. A., Dunn, N., Chen, D., Sabri, S., Torre-Ubieta, L. de la, Clark, A. T., Plath, K., Christofk, H. R., … Novitch, B. G. (2022). TGFβ superfamily signaling regulates the state of human stem cell pluripotency and capacity to create well-structured telencephalic organoids. *Stem Cell Reports*, *17*(10), 2220. https://doi.org/10.1016/J.STEMCR.2022.08.013

Deepthi Muthukrishnan, S., Qi, H., Wang, D., **Elahi, L**., Pham, A., Alvarado, A. G., Li, T., Gao, F., Kawaguchi, R., Lai, A., & Kornblum, H. I. (n.d.). *Low- and high-grade glioma endothelial cells differentially regulate tumor growth*. https://doi.org/10.1101/2023.07.07.548125 (in review)

Chapter 1

INTRODUCTION

Glioblastoma (GBM) is the most common and aggressive form of primary brain tumor in the central nervous system. The average survival rate of a glioblastoma patient is 15-18 months with treatment. Tumor heterogeneity and therapeutic resistance are two of the biggest challenges to developing effective treatments for glioma patients. In 2016, the world health organization (WHO) categorized central nervous system (CNS) tumors into distinct subtypes by incorporating both histopathological and molecular characteristics. Diffuse gliomas with mutation in the metabolic gene isocitrate dehydrogenase (IDH) gained its own special category. With the 2021 WHO revisions, adult diffuse gliomas are now either defined as IDH wildtype (WT) or IDH mutant (MT) astrocytoma and or IDH WT or IDH MT oligodendroglioma. Grade II/III IDH MT astrocytoma often harbors mutation in the tumor protein 53 (TP53) and alpha-thalassemia and (ATRX) genes and have intact cyclin-dependent kinase inhibitors 2A and 2B (CDKN2A/B). Grade IV IDH MT astrocytoma on the other hand has CDKN2A/B deletion along with TP53 and ATRX mutations. Oligodendroglioma are generally grade II/III and has the short arm of chromosome 1 and the long arm of chromosome 19 (1p/19q) co deleted.

IDHs are $NADP^+$ dependent enzymes that catalyze oxidative decarboxylation of isocitrate to α-ketoglutarate and reduce $NADP^+$ to NADPH. There are three isoforms of IDH: IDH1, IDH2, & IDH3. IDH1 is localized in the cytosol and peroxisome and plays important roles in glucose sensing, lipid and glutamine metabolism, and maintenance of cellular redox state. IDH2 and IDH3 are localized in the mitochondria. IDH2 is involved in glutaminolysis, ROS homeostasis and can protect cells from radiation, high glucose and heat shock induced apoptosis. IDH3 on the other hand is dependent on NAD and catalyzes the irreversible conversion of isocitrate to alpha ketoglutarate (α-KG).

Table 1: Common IDH mutations in gliomas

GENE	AMINO ACID SUBSTITUTION	% IN GLIOMAS
IDH1	R132H	89.3
IDH1	R132C	3.9
IDH1	R132S	1.5
IDH1	R132G	1.3
IDH1	R132L	0.3
IDH2	R172K	2.7
IDH2	R172M	0.8
IDH2	R172W	0.7

Arginine (R) residues in the IDH gene are crucial for sensing isocitrate and is commonly mutated in gliomas. About 90% of mutations in IDH1 is a single amino acid substitution at position 132 from R to H (histidine) and the other 10% to C (cysteine), S (serine), G (glycine), and L (leucine). Substitution to K (lysine), M (methionine) and W (tryptophan) is mostly seen at residue 172 of IDH2 (table1). IDH mutations are believed to be one of the earliest perturbations in low grade gliomas and patients usually have better disease prognosis due to the slower rate of tumor progression. Nonetheless, the IDH mutant tumors undergo malignant transformation, and the patients eventually succumb to tumor recurrence. Mutation in the IDH gene is a gain of function mutation that reduces α-KG to 2-hydroxyglutarate (2-HG) while converting NADPH to $NADP^+$. The concentration of 2-HG in gliomas (II-III) can range between 1mM-30mM and can alter a variety of cellular pathways. The most well-known effect of 2-HG pertains to DNA and histone modification. Besides epigenetic reprogramming, 2-HG has been reported to alter hypoxia-inducible factor signaling, differentiation, DNA repair, RNA methylation, mTOR pathway, immune microenvironment, and lipid metabolism. In the next sections I will expand more on the impact of IDH mutation and 2-HG on the epigenome and the lipidome.

THE EPIGENOME

DNA methylation

CpG island methylation

In 2010, Noushmehr et al. first analyzed promoter DNA methylation alteration in a large cohort of GBM samples and identified IDH MT tumors to have a distinct glioma CpG island methylator phenotype (G-CIMP)[1]. Further work from the same group analyzed DNA methylation level between primary and recurrent glioma samples and found that at recurrence, a subset of IDH MT tumors lost DNA methylation and transformed from a high G-CIMP to a low G-CIMP phenotype[2]. They compared transcriptome with the methylome and found an inverse relationship between gene transcription and methylation. However, only 19% of the genes downregulated in IDH MT tumors also had promoter hypermethylation suggesting that multiple epigenetic mechanisms are involved in transcriptional gene repression in IDH MT gliomas. Disruption in CCCTC-binding factor (CTCF) binding due to DNA methylation may offer one possible explanation for aberrant gene expression in IDH MT glioma. Flavahan et al. found that insulator dysfunction allowed enhancer FIP1L1 to aberrantly interact with the promoter of PDGFRα and upregulate its expression[3]. A more recent study using single cell multiomics identified intratumor DNA methylation heterogeneity in both IDH WT and MT tumors[4]. They found in both IDH MT high and low G-CIMP tumors enhancers pertaining to cell differentiation were mostly hypermethylated. Together this suggests a rather complex and heterogenous DNA methylation landscape in IDH MT tumors. DNA methylases and DNA methyltransferases are two main categories of enzymes that regulate DNA methylation and hence following this discovery several groups tried to understand whether function of these enzymes are altered in IDH MT gliomas.

DNA demethylases

Ten-eleven translocation (TET) enzymes are α-KG dependent dioxygenases that catalyze the oxidation of 5-methylcytosine (5-mC) into 5-hydroxymethylcytosine (5-hmC) and are important for cellular differentiation and cytosine demethylation. 2-HG competitively inhibits α-KG dependent dioxygenases and decreases 5-hmc by inhibiting tet1 and tet2[5]. Xu et al. analyzed IDH MT glioma samples and reported lower 5-hmc in IDH MT compared to IDH WT samples[6] . In acute myeloid leukemia disruption of tet2 impaired differentiation and promoted stemness[7]. One group tried to model low grade IDH MT gliomas by introducing R132H, shP53 and shATRX in neural stem cells and found that disruption of CTCF occupancy transcriptionally blocked SOX2 and inhibited differentiation[8]. Interestingly, subset of IDH WT GBM also has lower 5-hmc, and in this context SOX-2 was found to inhibit tet2 and decrease 5-hmc[9] suggesting distinct regulation of 5-hmc in IDH WT and MT tumors. What are the consequences of targeting TET2/SOX2 axis in IDH MT glioma model is still an open question. Although 2HG has been proposed to inhibit tet2, IDH MT tumor samples have been reported to express high transcript level of SOX2[10]. Targeting TET2/SOX2 axis to promote differentiation may be an interesting strategy for IDH MT gliomas.

DNA methyltransferases

DNA methyl transferases DNMT1, DNMT3A & DNMT3B catalyze the addition of methyl groups to cytosine residues of CpG nucleotides[11]. In an IDH1 R132Q knock in model 2-HG was found to directly bind to DNMT1 and affect gene expression[12]. Two studies have explored the effect of targeting DNMTs via 5-azacytadine and decitabine in IDH MT glioma with the goal of promoting demethylation and inducing differentiation. Decitabine reduced genome-wide DNA methylation and promoted glial differentiation in IDH MT glioma cells[13]. 5 azacytidine transcriptionally activated GFAP and in combination with temozolomide improved survival in IDH1 R132H glioma[14]. 5-azacytidine induced differentiation of IDH MT glioma cells only with longer

treatment. Perhaps combining drugs to promote differentiation earlier would be a better way of targeting IDH MT gliomas.

Histone Methylation

Histone demethylases

Histone demethylases are the second group of α-KG dependent dioxygenases inhibited by 2-HG. Turcan et al. first demonstrated that overexpressing IDH1 R132H in astrocytes increased histone methylation[15]. Later, Chao Lu et al. showed inhibition of Jumonji-C domain histone demethylase KDM4C was sufficient to increase histone 3 lysine 9 tri-methylation (H3K9me3) and block differentiation[16]. Interestingly, they found lipid droplets were markedly reduced in IDH MT cells indicating an interesting connection between the epigenome and the lipidome. Recently, Gunn et al. using CRISPR-screen found that KDM5 family of demethylases KDM5A, KDM5C, and KDM5D are inhibited by (R)-2HG and plays a role in pathogenesis of both IDH MT AML and IDH MT glioma[17]. Lastly, the histone methylome may be distinct in IDH MT astrocytoma versus IDH MT oligodendroglioma. IDH MT astrocytoma have increased mark compared to IDH MT 1p/19q co deleted oligodendroglioma[18]. This suggests IDH MT astrocytoma may be more sensitive to histone demethylase inhibitors than oligodendrogliomas.

Histone Deacetylation

Histone deacetylases

Histone deacetylases (HDACs) are zinc dependent enzymes and whether 2-HG directly or indirectly interferes with enzymatic function of HDACs is not known. A proteomics study reported that overexpression of IDH1 in normal human astrocytes increased histone methylation and concurrently decreased histone acetylation at several histone residues with the most significant decrease in histone acetylation at H3K4 and H3K9, two marks associated with transcriptional

repression[19]. This suggests HDACs by mediating deacetylation may be involved in downregulation of genes in IDH MT gliomas. Another study analyzed mRNA and protein expression of HDACs in low- and high-grade astrocytoma patient samples and found that expression of class II and class IV HDACs were higher in low grade astrocytoma compared to GBM[20]. GBM samples also had increased H3K27 acetylation compared to low grade gliomas. This study did not report the IDH status of the samples analyzed but since the majority of low-grade gliomas are IDH MT, one can postulate that to maintain a repressive chromatin state IDH MT gliomas need to maintain low level of histone acetylation. Garrett et al. recently reported overexpression of IDH1 resulted in a hypoacetylation phenotype[21]. They also reported HDAC 1-4, and HDAC6 were highly expressed in IDH1 MT patient samples and knockdown of HDAC1 and HDAC6 diminished tumor invasiveness in vivo. This suggests HDACs are potentially important targets for IDH MT gliomas as HDACs are known to affect gene expression, chromatin, cell cycle, differentiation, metabolism, apoptosis and many more processes in cancer cells.

HDAC inhibitors

HDAC inhibitors (HDACis) increases histone acetylation and exert anti-tumor effects through multiple molecular mechanisms such as cell cycle arrest, extrinsic and intrinsic apoptosis, metabolism, senescence, tumor angiogenesis, and modulation of immune response to name a few. Most pan-HDACi target class I, II and IV HDACs but many selective HDACis are also available. The results with HDACis in IDH MT glioma models are currently a mixed bag. Kim et al. reported R132H overexpression in U87 and U373 caused resistance to HDACis by increasing NANOG through epigenetic mechanism[22]. Chang et al. overexpressed R132H in NHA and LN229 cell lines and reported R132H mutation made the cell lines more sensitive to HDACi, belinostat[23]. Kayabolen et al. on the other hand reported H3K27me3 demethylase inhibitor GSK-J4 in combination with belinostat was more effective against IDH MT gliomas but did not specify whether belinostat as a monotherapy is effective or not[24]. Lastly, Sears et al. reported IDH MT

glioma cells are more sensitive to HDACis panobinostat and VPA[25]. These studies suggest IDH MT gliomas may respond to more than one HDACi. However, how effective HDACis are in vivo and whether they work through any unique mechanism in IDH MT glioma is still not very clear.

The Chromatin State in IDH1 MT

What is the impact of histone modifications and DNA methylation on the chromatin state of IDH MT gliomas? Is the chromatin in IDH1 MT more “closed” simply because these tumors have increased histone and DNA methylation? Recent studies suggest the answer is not that simple. Using a doxycycline inducible R132H immortalized human astrocytes (IHAs) model, Turcan et al. demonstrated the impact of R132H mutation on histone modifications, and ultimately on the overall chromatin landscape is quite dynamic[26]. R132H MT IHAs had enrichment of both active (H3K4me3) and repressive (H3K9me3) marks. Although there was an overall increase in repressive histone marks in IDH1 MT compared to WT parental cells the overall proportion of these marks were similar in parental and IDH1 MT glioma cells. This suggests epigenetic changes in IDH1 MT are region specific. Another study using single nuclei ATAC-seq identified that transcription factors and non-coding RNAs have differential accessibility in low grade IDH MT co-deleted versus non co deleted gliomas[27]. Finally, grade (IV) recurrent IDH MT tumors were found to have fewer ATAC seq peaks compared to primary IDH WT tumor samples suggesting the chromatin condensation in MT tumors[28]. Together these studies suggest that the chromatin landscape of IDH MT gliomas are both heterogenous and dynamic. Focusing on regional epigenetic differences and how they ultimately affect gene expression will help narrow down the search for the most effective epigenetic drugs for IDH MT gliomas.

THE LIPIDOME

Cellular lipids are molecularly diverse, complex, and dynamic. Over 50,000 different lipid species have been identified till now. Lipids are important signaling molecules, essential for cellular growth and energy storage, and are essential building blocks for cellular membrane. GBM are highly proliferative cells and utilize different lipids for cellular growth and survival. Fatty acids, phospholipids, triglycerides, and sterols are some of the major lipid classes that have been reported to be altered in IDH MT gliomas. In the next sections I will review what we know so far about the fatty acids, phospholipids, & sterols specifically in IDH MT gliomas.

Fatty Acids

Saturated & Unsaturated fatty acids

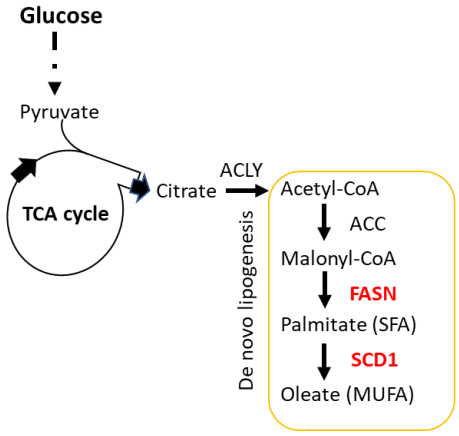

Figure 1: Simplified de novo lipogenesis pathway. Tricarboxylic acid cycle(TCA); Enzyme abbreviations: ATP Citrate Lyase (ACLY), Acetyl-CoA carboxylase (ACC), Fatty Acid Synthase (FASN), Stearoyl-Coa Desaturase (SCD).

In the cytosol and the peroxisome WT IDH1, and in the mitochondria WT IDH2 reduces $NADP^+$ to NADPH, which is then used for fatty acid synthesis or to prevent oxidative stress[29]. Fatty acid synthase (FASN) is a NADPH dependent enzyme that is responsible for de novo palmitate (saturated fatty acid) synthesis. IDH MT cells are thought to have defective palmitate synthesis capability. Using human colorectal carcinoma cells HCT119 and NHA R132H overexpression

model Gelman et al. showed that IDH1 MT have reduced capacity to produce NADPH and instead use the pentose phosphatase pathway to generate NADPH which is primarily used to synthesize 2-HG[29]. Interestingly, even at the expense of other NADPH requiring pathways such as the de novo lipogenesis pathway (figure 1) that are essential for cell growth, IDH1 MT cells preferred using NADPH for synthesis of 2-HG rather than using it to synthesize palmitate. A separate study overexpressed R132C in fibrosarcoma cell line and found similar results showing that de novo lipogenesis in IDH1 MT is altered at the expense of 2HG production[30]. Surprisingly, supplementation of exogenous palmitate led to 20% more production of 2-HG, suggesting in the presence of exogenous palmitate more NADPH is available for 2-HG synthesis. Finally, Gelman et al. showed that IDH1 MTs were more dependent on acetate for palmitate synthesis. Different tumors may have different metabolic requirements and it is unclear whether de novo lipogenesis pathway is a vulnerability of IDH MT gliomas. Bleeker et al. analyzed IDH1 MT GBM tissue and concluded NADPH production is reduced by 38% in IDH MT GBM[31]. IDH MT Grade IV astrocytoma tissue has also been reported to have an increased ratio of monounsaturated to saturated fatty acid suggesting potential decrease in saturated fatty acid synthesis in IDH MT Grade IV astrocytoma[32]. Lita et al. overexpressed R132H and R132C mutations in U251 cell line and found that $U251^{WT}$ was more sensitive to FASN inhibition than $U251^{R132H}$ and $U251^{R132C}$[33]. In our lab we overexpressed R132H mutation in U87 and found that overexpression of R132H in U87 does not faithfully recapitulate the features of IDH MT tumors. So, whether IDH MT gliomas are sensitive to FASN inhibition may still be a question that needs further investigation. Interestingly, Lita et al. showed patient derived IDH1 MT cell lines had higher FASN protein expression than IDH WT but did not report whether the patient derived IDH MT lines were sensitive or resistant to FASN inhibition. FASN has been investigated as therapeutic target in various types of cancers[34]. Extracellular vesicles from GBM patients have been found to be enriched in FASN compared to healthy patients[35].FASN inhibition has been shown to inhibit

vascularization [36], stemness[37], and promote apoptosis[38]. in WT glioma cells. However, knowledge on how FASN inhibition rewires the lipidome in both WT and MT GBM is scarce and requires more investigation.

Stearoyl-CoA-desaturase (SCD) is the primary enzyme in the de novo lipogenesis pathway that is responsible for synthesis of oleic acid, a monounsaturated fatty acid. 2-HG increases protein expression of SCD1 and SCD5 in IDH MT cells. 2-HG and increased amount of oleic acid synthesized by SCD is responsible for endoplasmic reticulum (ER) and Golgi dilation in IDH MT cells[33]. Lita et al. showed that IDH MT glioma cells are more sensitive to oleic acid-induced apoptotic cell death. What happens if you inhibit SCD in IDH MT is not known but high amount of monounsaturated fatty acids in MT tissue[32] might indicate SCD dependency in DH MT GBM. Inhibition of SCD in WT GBM cells has been found to inhibit tumor growth by promoting lipotoxicity[39]. Whether polyunsaturated fatty acids influence growth of IDH MT gliomas is still not known. However, several polyunsaturated fatty acids such as arachidonic acid (AA), eicosapentaenoic acid (EPA)[40] and docosahexaenoic acid (DHA)[41] have been found to inhibit growth of WT GBM cells through autophagy and apoptosis. Understanding the vulnerability of IDH MT glioma cells to different saturated and unsaturated fatty acids will inform us better how to exploit the lipidome and therapeutically target IDH MT gliomas.

Phospholipids

Phospholipids are important components of cell membranes and perform a wide variety of functions ranging from signal transduction to inflammatory response[42]. Malignant cell transformation and tumor progression are generally associated with higher phospholipid content [43]. Multiple studies to date have shown that phospholipids are altered in IDH MT glioma samples. Phosphocholine (PCho) and Glycerophosphocholine (GPCho) were found to be higher in IDH1^{R132H} MT compared to respective IDH WT in cultured cells, xenograft, and patient tissue

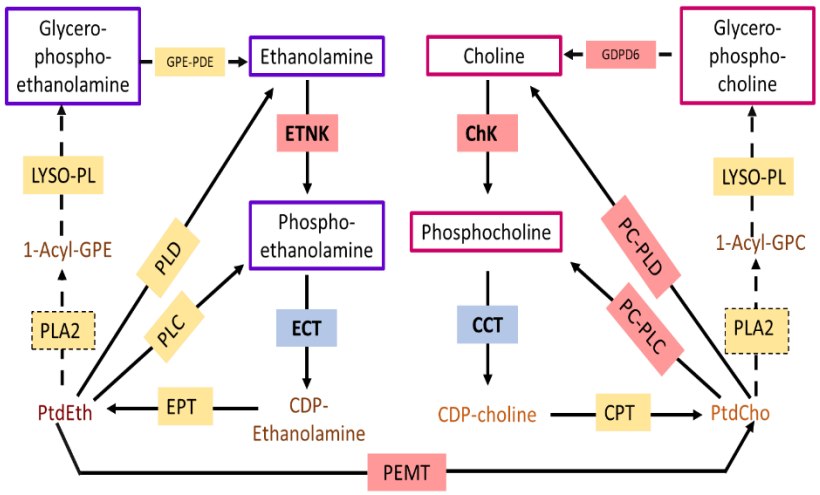

Figure 2: Crosstalk between Ethanolamine and Choline Pathway

Shaded boxes indicate enzymes. Metabolite abbreviations: 1-acyl-GPE, 1-acyl-glycerophosphoethanolamine; 1-acyl-GPC, 1-acyl-glycerophosphocholine; PtdCho, phosphatidylcholine; PtdEth, phosphatidylethanolamine; Enzyme abbreviations: CCT, phosphocholine cytidylyltransferase; ChK, choline kinase; CPT, diacylglycerol cholinephosphotransferase; CTL, choline transporter-like protein; EtT, ethanolamine transporter; ECT, phosphoethanolamine cytidylyltransferase; EPT, diacylglycerol ethanolaminephosphotransferase; ETNK, ethanolamine kinase; GPE-PDE, glycerophosphoethanolamine phosphodiesterase; GDPD6, glycerophosphodiester phosphodiesterase domain containing 6; lyso-PL, lysophospholipase; PEMT, phosphatidylethanolamine N-methyltransferase; PLA2, phospholipase A2; PLC, phospholipase C; PLD, phospholipase D

biopsies (PTB)[44]. Fack et al. found phosphatidylinositol was also higher in IDH1 MT PDX model[45]. However, in one study with human oligodendroglioma (HOG) cells phosphocholine was lower in MT compared to wildtype[46]. In contrast $IDH2^{R172K}$ cells had lower PCho and GPCho levels[46]. Phosphoethanolamine is another phospholipid that has been found to be consistently lower in both IDH1 MT patient derived xenograft (PDX) and PTB[44]. What are the consequences of alteration of phosphocholine, and ethanolamine is IDH MT gliomas? Most studies reported alteration in these metabolites but did not show how functionally these alter cancer phenotypes. Interestingly, Viswanath et al. reported endoplasmic reticulum (ER)-phagy was responsible for lower phosphatidylcholine (PtdCho) and phosphatidylethanolamine in IDH MT gliomas[47]. 2-HG

inhibited the activity of choline kinase (ChK) and ethanolamine kinase (ETNK), and the activity of these enzymes could be rescued by treatment with IDH MT inhibitor[47]. There is a significant crosstalk between the ethanolamine and choline pathways as summarized in (figure 2) and increase in phospholine may be driving phosphoethanolamine down or vice versa. The two pathways and whether targeting the enzymes in these two pathways is a vulnerability in IDH MT gliomas need further investigation.

Sterol

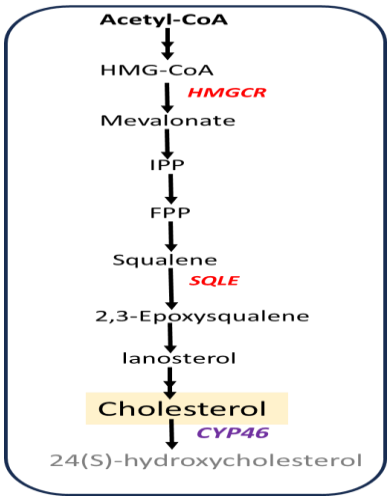

Figure 3: Simplified de novo cholesterol biosynthesis pathway.

HMG-CoA reductase (HMGCR) and squalene epoxidase (SQLE) are the two rate limiting enzymes in the pathway. IPP: Isopentenyl-PP, FPP: Farnesyl-PP, CYP46: cholesterol 24-monooxygenase

The Sterol Regulatory Element-Binding Proteins (SREBPs) are major transcriptional regulators of the cholesterol biosynthesis pathway. There are two rate limiting enzymes in the cholesterol biosynthesis pathway: 3-hydroxy-3-methylglutaryl coenzyme A reductase (HMGCR) and squalene monooxygenase (Figure3) [48]. Overexpression of R132H in U87 has been found to activate SREBP1 pathway and promote proliferation of cells[49]. IDH1 MT glioma cells have lower cholesterol content but increased production of 24(S)- hydroxycholesterol which is mediated by

the enzyme cytochrome P450 46A1(CYP46A1). Increase in 24(S)- hydroxycholesterol results in low-density lipoprotein receptor degradation and lowers cholesterol influx into cells. On the other hand, Upregulation of ATP-binding cassette transporter A1 (ABCA1), ABCG1, and apolipoprotein E (ApoE) promotes cholesterol efflux in IDH MT gliomas. Interestingly, secretion of excess cholesterol by IDH MT gliomas have been found to polarize microglia cells to acquire a proinflammatory (M1) phenotype(T. Wang et al., 2023); however, the authors did not discuss how this influences the tumor immune environment. How cholesterol metabolism affects function of immune cells in IDH1 Mts may be an interesting area of study. Lastly, R132H MTs have been found to have increased sensitivity to HMGCR inhibitor atorvastatin [51].

Conclusion

IDH mutations rewire both the epigenome and lipidome and the changes associated with it are both heterogenous and dynamic. A lot of effort till date has been focused on profiling epigenetic and lipidomic changes in patient tissue, PDX, mouse models, and various IDH MT cell culture models. However, in IDH MT glioma how does DNA methylation or histone acetylation/methylation affects function of lipogenic enzymes is not really known. Lipid composition can directly affect chromatin proteins. For instance, palmitoylation, a lipid modification where palmitate is added to a cysteine residue can affect tetramer formation of H3 and H4 and ultimately affect the overall chromatin structure and transcription. On the flip side epigenetic modification like acetylation can directly affect lipogenic enzyme FASN by promoting its degradation via the ubiquitin-proteosome pathway. Epigenetic gene regulation is already complex and adding lipid modifications to the mix only adds to the complexity. Untwining the intricacies of lipid and epigenome modification may ultimately get us close to curing IDH MT gliomas.

Modeling of IDH1 MT Glioma

One of the biggest challenges in studying IDH MT gliomas is that it is difficult to grow in vitro and in vivo. Currently, there is no consensus as to what the best way is to model IDH MT low- and high-grade gliomas. Overexpression of R132H mutation in either immortalized human astrocytes (IHA)[15] and or in WT GBM cell line U87[49,52] are two of the most common ways researchers try to study IDH MT gliomas. Overexpression of R132H mutation in IHA results in cellular transformation but does not really make a tumor in vivo[53] . On the other hand, U87 tumors are not as invasive, lack intratumoral heterogeneity, and authenticity of the cell line has been challenged making U87 not quite a suitable model to study either WT or MT gliomas[54]. For instance, there are conflicting reports as to whether IDH MT gliomas are more sensitive[55] or resistant[22] to HDACis and studies reporting these results used a U87-R132H overexpression model. Lastly, overexpression of only R132H mutation does not consider the other genetic alterations such as p53 and ATRX that are commonly seen in IDH MT astrocytoma and or oligodendroglioma.

In recent years, several groups have moved towards creating genetically engineered mouse glioma model with multiple genetic mutations to better recapitulate the biology of IDH MT tumors. In 2019, Nunez et al. created a genetically engineered mouse model harboring IDH1R132H, TP53 and ATRX inactivating mutations, and activating NRAS-G12V mutations[56]. The mouse MT IDH1 (mMTIDH1) model exhibited increased survival, increased H3 hypermethylation, and blocked oligodendrocyte differentiation[57]. Similar, to what we have seen in primary IDH MT GBM cell lines[58] they found mMTIDH1 model was radioresistant. This model recapitulates several features of patient tumors, but the primary limitation is that the activating NRAS mutation is generally not seen in IDH1 MT gliomas.

Shi et al. in 2022 came up with another genetically engineered mouse model for grade III astrocytoma. They engineered a mouse model with R132H/p53/ATRX/PIK3CA mutations[59]. This

model is better than the previous as PIK3CA alterations are seen in IDH MT gliomas. Nonetheless, only 10% of IDH1 MT tumors have PIK3CA alterations.

More recently, Abdullah et al. created a organoid model for low grade IDH MT gliomas by culturing low grade primary patient tissue in 5% oxygen. They reported low grade IDH organoids produced 2HG and maintained genetic alterations and molecular features of parental tumors over long culture period and after biobanking[60]. They, however, did not characterize the epigenome of these organoids. Whether these organoids form tumor xenograft in vivo currently is not known. However, the finding is exciting and gives hope to people who are studying IDH MT gliomas. Interestingly, this organoid model maintains non-tumor cells like endothelial and microglia which makes it a great system to study interaction between tumor-endothelial and tumor-microglia interactions in vitro.

Kornblum lab IDH MT GBM cell lines

In our lab we established and characterized several high grade IDH WT and IDH MT glioma cell lines[61]. The primary MT glioma cell lines in our lab express mutant R132H protein (Figure4A), Have high 2-HG (Figure4B), and exhibit a longer cell division time (Figure 4C). To assess genome wide methylation, we used reduced bisulfite sequencing and found that IDH MT glioma cultures are hypermethylated compared to IDH WT (Figure 4D). Micro-array data from our library of patient derived cell lines showed that our IDH MT glioma cell lines have a distinct gene repression profile compared to IDH WT glioma cell lines (Figure 4E). Several of the top genes reported by Noushmehr et al.[1] to be downregulated in IDH MT gliomas are also downregulated in our primary IDH MT cell lines (Figure 4F). Lastly, overexpression of R132H mutation in U87 does not recapitulate gene expression profile seen in primary IDH MT glioma cultures (Figure 4G).

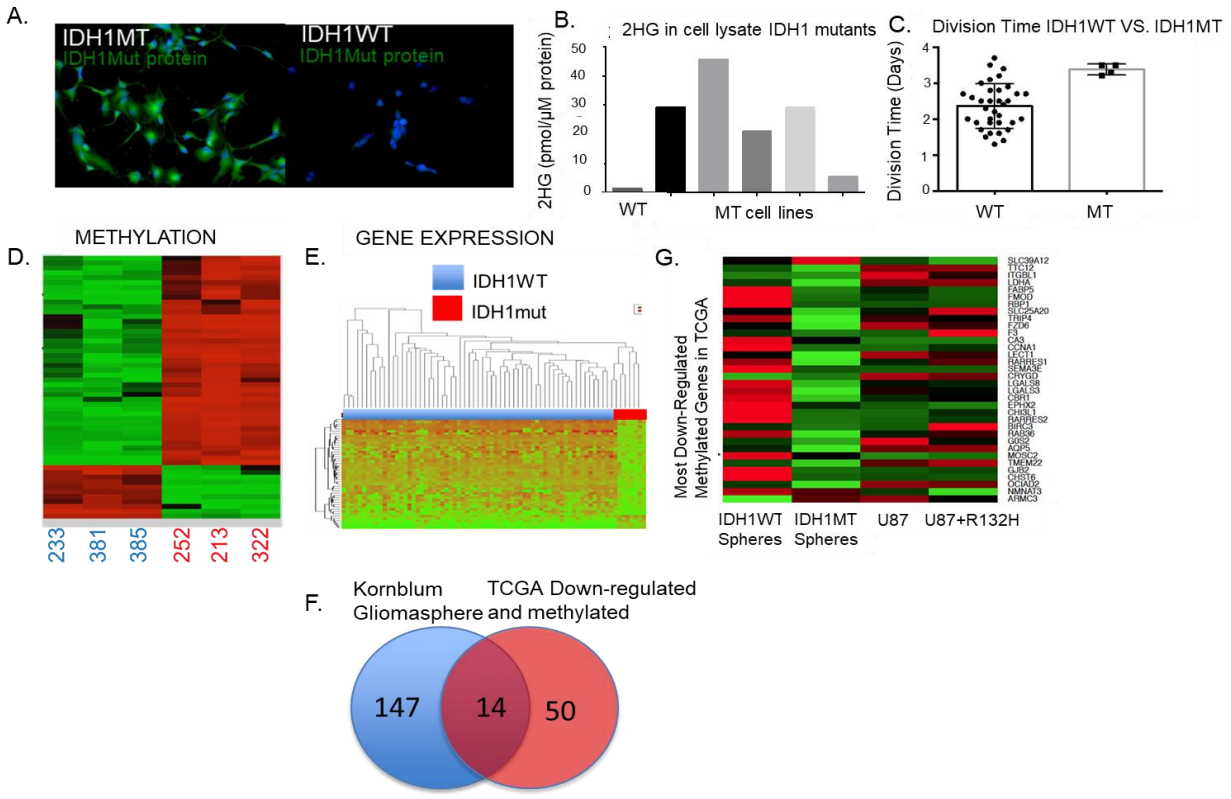

Figure4: Characterization of IDH MT glioma cell lines

A. Immunofluorescence staining of mutant IDH1 in a MT IDH and WT cell line

B. D-2G content in multiple cell lines

C. Cell division time in IDH MT versus IDH WT

D. Heat map showing differential methylation pattern in WT and MT cell lines

E. Micro-array data showing gene expression pattern in our library of WT and MT cell lines

F. Venn diagram comparing Kornblum spheres with TCGA methylated and downregulated genes.

G. Heat map comparing most downregulated and methylated TCGA genes in primary and R132H overexpression culture.

How important is R132H mutation or 2HG in high grade IDH MT glioma?

IDH1 mutation is thought to be a driver in early stages of gliomagensis and a passenger at later stages of disease[53]. Using two isogenic models where R132H mutation is the sole driver of cellular transformation Johannessen et al. showed that cellular transformation after introduction of R132H oncogenic insult happens within 3 days and is only reversible by prior exposure to a IDH MT inhibitor. Treatment with IDH inhibitor even as early as 4 days after oncogenic transformation is not enough to completely reverse some of the epigenetic changes such as histone methylation[53]. This suggests there is a relatively short therapeutic window to cure IDH MT gliomas with an IDH MT inhibitor that blocks 2-HG, and epigenetic changes become permanent quickly and cannot simply be reversed by removing 2HG. Another study by Moure et al. further supported this finding. Moure et al. took a patient derived heterozygous IDH MT cell line and using CRISPR/cas9 deleted the IDH WT allele and showed that even after removal of 2HG the cells-maintained DNA hypermethylation at several CpG sites[62] that were previously seen in the original parental heterozygous cell line. This suggests hypermethylation at some CpG sites also becomes permanent and cannot be simply reversed by removal of 2HG. The authors did note that the hemizygous cell line showed genome-wide DNA demethylation at open sea regions; however, this pattern of demethylation was similar to what is seen in G-CIMP low IDH MT patient tumor. This suggests loss of 2HG or loss of IDH WT allele that results in loss of 2HG does not necessarily make IDH MT tumor into a IDH WT tumor but rather make them more like a G-CIMP low IDH MT tumor that also maintains if not all but many of the same epigenetic alterations seen in heterozygous IDH1 MT glioma cell lines. One interesting observation that we and others have made is that heterozygous IDH MT cell lines tend to lose their heterozygosity in culture by either kicking out the WT or MT allele[63]. Mazor et al. performed copy number alterations (CNA) analysis of paired primary IDH MT gliomas and showed that a population of MT cells with IDH1 copy number alterations already existed in the parental tumor and is selected for in vitro[63]. They further

showed that selection for IDH1 CNA also happened in vivo in MT xenograft with serial passage of the tumor. Together this suggests hemizygous IDH MT cell lines are not necessarily irrelevant model for IDH MT gliomas but perhaps they represent a population of IDH MT cells that are less methylated and more aggressive.

Finally, to add to the observations that others have made we treated two of our heterozygous IDH MT cell lines HK252 and HK211 with 10μM of AGI-5198 (C35) for three weeks and conducted ATAC and RNA sequencing. We saw very little change in chromatin accessibility after 3 weeks of treatment with AGI-5198 (Figure5A). Pearson correlation analysis suggested that gene expression pattern with C35 is most similar to the control cells whereas in comparison we saw major changes in gene expression with two different HDACis VPA and LBH589 (Figure5B). RNA sequencing on multiple IDH WT and MT cell lines and PDX showed hemizygous BT142 and MGG119 cell lines cluster closer to heterozygous HK252 than any of the WT cell lines and PDX that were part of the analysis (Figure5C). Finally, we managed to test the effect of MT IDH inhibitor AG881 on multiple IDH MT glioma cell lines. Most cell lines did not show a significant change in growth with AG881 but HK213 (IDH1 R132H mutation) and GS026 (IDH2 mutation) grew faster after treatment with AG881.

In summary, we conclude IDH1 mutation plays a minor rather than a major role in high grade IDH MT. It is possible that in some cell lines IDH mutations have more of a role than other cells as we did see growth promoting effect in some cell lines. The chromatin and transcriptomic pattern after 2HG removal is not that much different and hemizygous MT cell lines still cluster closer to heterozygous MT cell lines. Therefore, we think both heterozygous and hemizygous cell lines can inform researchers about potential therapeutics for targeting IDH MT gliomas.

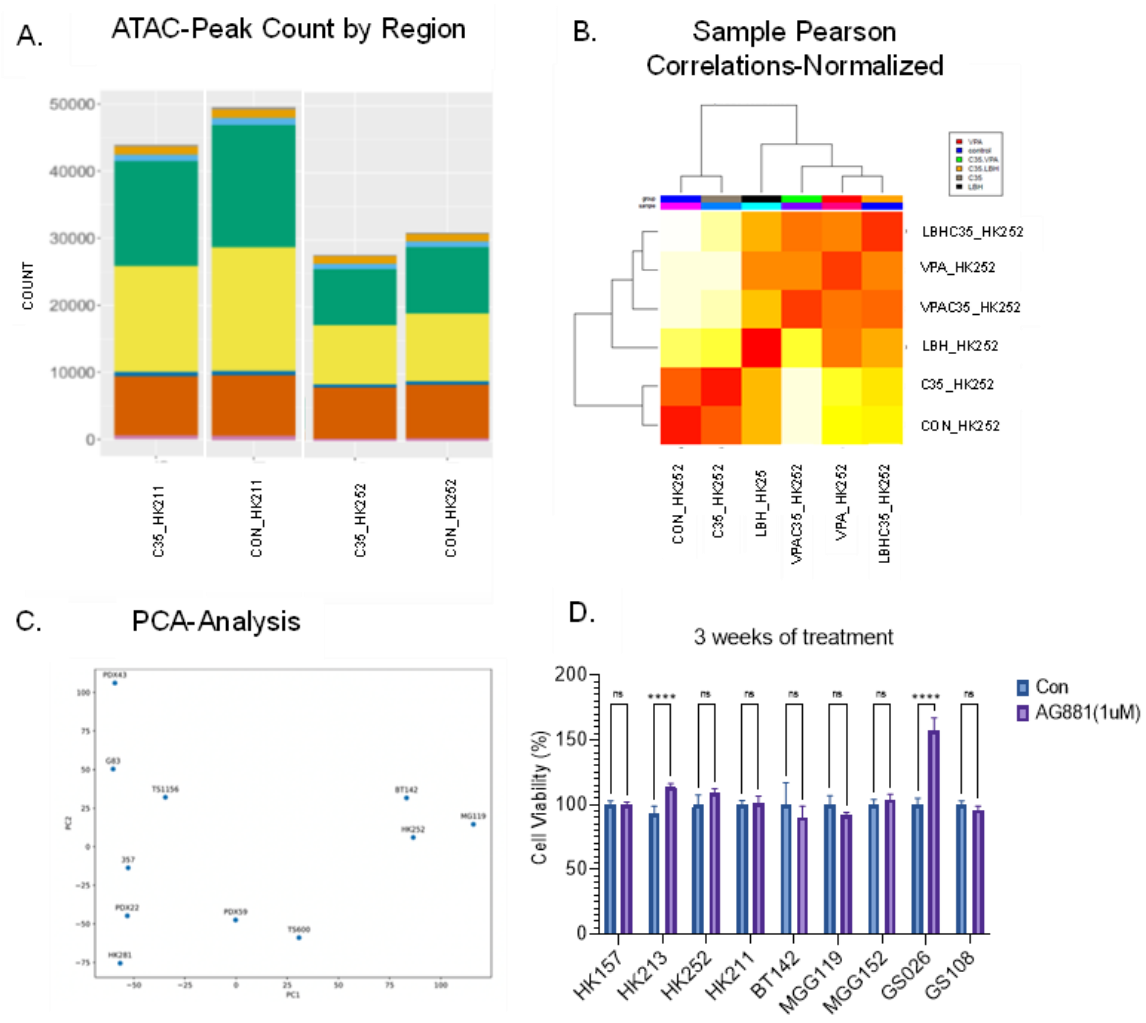

Figure5. IDH inhibitors have minimal effect on gene expression, chromatin, and growth of IDH MT glioma cell lines.

A. ATAC-seq peaks in HK252 and HK211after three weeks of treatment with C35.

B. Pearson correlation analysis in HK252 treated for 3 weeks with VPA, LBH589, and the combination.

C. PCA analysis on RNA seq data on multiple WT and MT cell lines. MT cell lines cluster to the right of WT cell lines.

D. Response of multiple IDH MT glioma cell lines treated for 2 weeks with AG881.

Chapter 2

De novo lipogenesis pathway is a vulnerability in IDH mutant glioma

Abstract

Histone deacetylases have multifaceted targets and can rewire both the chromatin and lipidome of cancer cells. In this study we show that valproic acid (VPA) an anti-epileptic and histone deacetylase inhibitor decreases promoter accessibility and inhibits transcription of multiple lipogenic genes in IDH MT but not IDH WT cells. We focus on one of the lipogenic candidates FASN and show that VPA targets FASN via the mTOR pathway. Both VPA and a selective FASN inhibitor TVB-2640 alters the lipidome and induces apoptosis in a IDH MT but not in a IDH WT cell line. Combination of VPA with TVB-2640 enhances lipotoxicity in vitro and VPA in combination with FASN knockdown significantly improved survival of mice in a IDH1 MT primary orthotopic xenograft model in vivo. We propose to prevent metabolic compensation, combination of VPA with FASN inhibitor may be a better way of therapeutically targeting IDH MT gliomas.

Introduction

Missense mutation in the gene isocitrate dehydrogenase (IDH) reprograms the metabolic and epigenetic landscape of IDH mutant (MT) gliomas making them distinct from IDH wildtype (WT) gliomas. WT IDH catalyzes the conversion of isocitrate to alpha-ketoglutarate (α-kg) whereas MT IDH reduces α-kg to the oncometabolite 2-hydroxyglutarate (2-HG). 2-HG blocks enzymatic function of ten-eleven translocation (TET) family of 5-methylcytosine (5mC) hydroxylases, and Jumanji family of histone demethylases resulting in an increase in both histone and DNA methylation[15,16]. Hence, inhibitors that directly target MT IDH and block 2-HG have been popular targets for IDH MT gliomas but when tested in vitro and in vivo settings have produced fruitless or mixed results[64–67]. Chromatin modifying drugs such as histone deacetylase inhibitors (HDACis) are promising candidates for gliomas and have been shown to inhibit growth of glioma by multiple mechanisms such as cell cycle arrest, apoptosis, demethylation, and metabolic rewiring[68–70].

Broad spectrum HDACis target histones and alter the chromatin but can also target non-histone proteins which in an HDAC dependent or independent manner can alter cellular signaling and metabolism[68]. In recent years, one non histone protein that has emerged as an interesting target of HDACis is fatty acid synthase (FASN). FASN is a key enzyme in the de novo lipogenesis pathway and catalyzes the synthesis of palmitate from acetyl-coA, malonyl-coA and nicotinamide adenine dinucleotide phosphate (NADPH). Acetylation destabilizes FASN and promotes FASN degradation via the ubiquitin-proteosome pathway which in turn can inhibit proliferation of tumor cells[71]. HDAC3 has been identified by two independent studies to be responsible for deacetylation of FASN[71,72].

IDH MT tumors have reduced ability to produce NADPH. High 2-HG in IDH MT tumors are thought to consume NADPH and limit the availability of NADPH for de novo lipogenesis[29,73]. Tumors with R132H mutation are thought to have defective palmitate synthesis capacity making

them more vulnerable to oxidative stress[74] .FASN is a NADPH dependent enzyme and whether IDH MT gliomas have a vulnerability to FASN inhibition is not clear.

In this study, we set out to explore the vulnerability of IDH MT glioma to HDACis thinking that the unique methylated epigenome and repressed transcriptome of IDH MT glioma would make them more vulnerable to HDACis since HDACis are generally thought to increase gene transcription and result in chromatin decondensation. We found that IDH MT glioma cell lines responded to multiple HDAC inhibitors but were particularly sensitive to VPA treatment. VPA treatment activated transcription of a large number of genes, but this was largely associated with a condensed chromatin state. We found a significant loss of chromatin accessibility at promoters of multiple lipogenic genes. We focused on one of those candidate genes FASN and show that both VPA treatment and FASN inhibition by a selective FASN inhibitor TVB-2640 rewires the lipidome and promotes apoptosis in a IDH MT but not IDH WT cell line. VPA itself targeted FASN via inhibition of the mTOR signaling pathway but it's effect on the lipidome was distinct from TVB-2640 which we think is primarily because of VPA's multiple lipogenic targets. Lastly, we show that in a primary IDH MT xenograft model combination of FASN knockdown with VPA significantly improved survival of mice compared to FASN knockdown or VPA alone.

Results

IDH MT glioma are sensitive to VPA in vitro and in vivo

We tested three different HDACis VPA, panobinostat (LBH589), and belinostat (PXD101) in varying concentrations in two IDH WT and three IDH MT primary glioma cell lines. All three MT cell lines had higher 2HG than IDH WT cell lines (Fig1F). Although BT142 is hemizygous for R132H mutation the 2HG amount is still double than the IDH WT cell lines tested. Both IDH WT and IDH MT cell lines responded to panobinostat and there was no significant difference in the IC50 or hill slope between the two dose response curves (Fig1B). IDH WT cell lines were more sensitive to belinostat (IC50, 0.84; hill slope -0.54) than IDH MT glioma cell lines (IC50, 1.97; hill slope -0.82) (Fig1C). IDH MT glioma cell lines were more sensitive to VPA > 1mM (IC50, 0.96; hill slope -1.68) than IDH WT (IC50, 1.23; hill slope -0.80) (Fig1A).

We further tested the effect of belinostat and VPA in a syngeneic mouse IDH1 (mIDH1) glioma cell culture model. The mIDH1 MT cell line NPAIC1((NRAS/IDH1^{R132H}/shP53/shATRX) had higher 2HG than mIDH1 WT cell line NPAC54B (NRAS/shP53/shATRX) and treatment with MT IDH inhibitor AG881(1μM) blocked 2HG production (Supplementary Fig 1D). NPAIC1 had a lower IC50 for both VPA (IC50, 1.37 and belinostat (IC50, 0.28) compared to NPAC54B, VPA (IC50, 1.64) and belinostat (IC50, 0.57) respectively(Fig1D, 1E) However, NPAC54B had a steeper hill slope for both VPA (Hill slope -2.6)(Fig1D) and belinostat (hill slope -2.19) compared to NPAIC1, VPA (hill slope -1.22) and belinostat (hill slope -0.87) respectively (Fig1D, 1E).

We next tested the effect of VPA in vivo. Most of our heterozygous primary IDH MT glioma cell lines do not have the ability to form xenograft in vivo, hence we tested the efficacy of VPA in vivo in the syngeneic mIDH1 MT glioma model and primary IDH MT cell line BT142. VPA (300mg/kg; twice daily) treatment slowed down tumor growth (supplementary Fig1A) and significantly improved survival of mice bearing NPAIC1 tumor xenografts (Fig1F) but did not slow

down tumor growth (supplementary Fig1B) or improve survival of mice bearing NPAC54B tumor xenografts (Fig1D). Treatment with AG881(2mg/kg; twice daily) in combination with VPA decreased survival of mice bearing NPAIC1 tumor xenografts compared to VPA alone (Supplementary Fig1E) but had no effect on mice bearing NPAC54B tumor xenografts (Supplementary Fig1E). VPA treatment also slowed down tumor growth (supplementary Fig1C) and significantly improved survival of mice bearing BT142 tumor xenografts (Fig1E). Together, we conclude IDH1 MT are sensitive to VPA in vitro and in vivo.

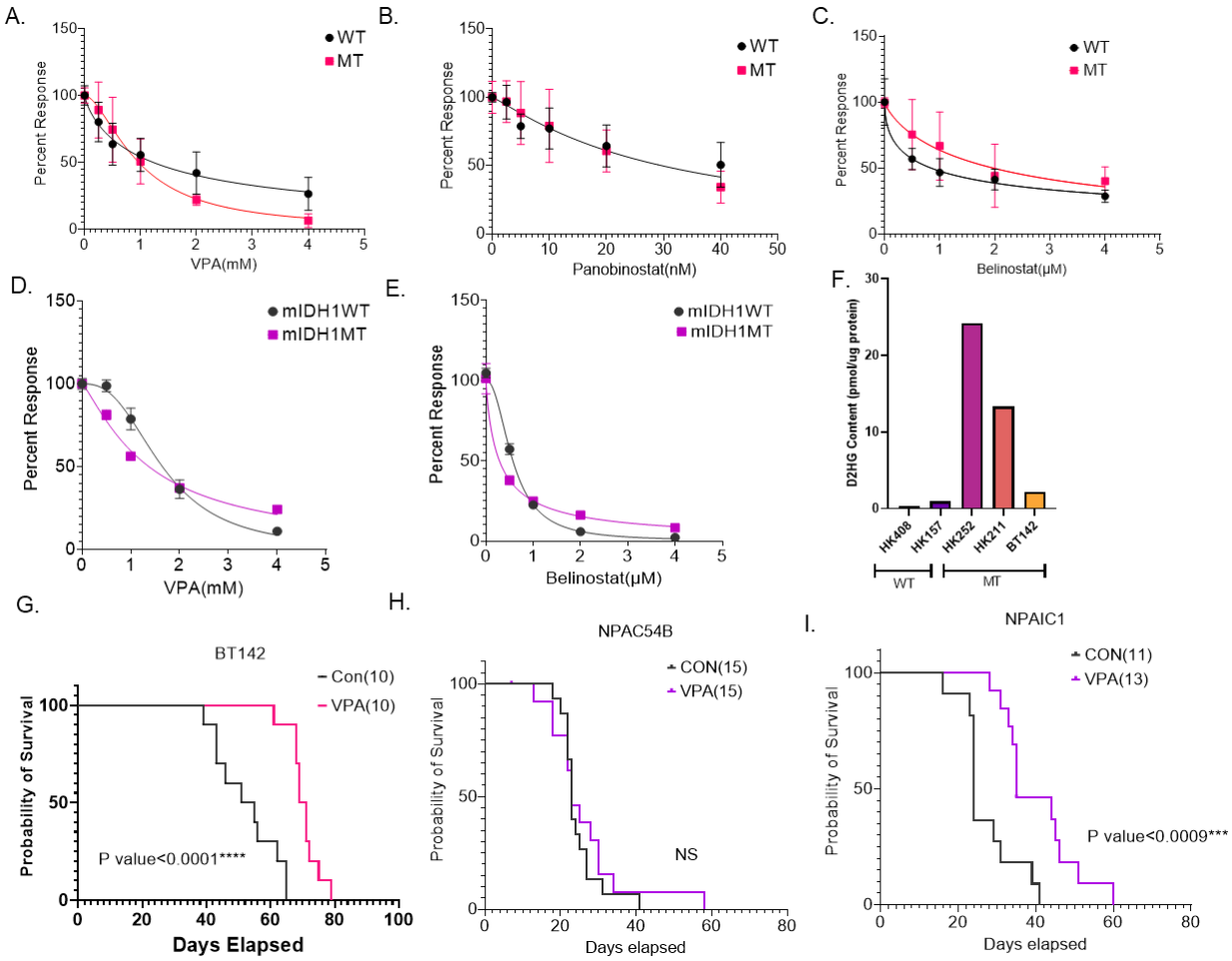

Fig1: IDH MT glioma cell lines are sensitive to VPA in vitro and in vivo

A-C Dose response curve of IDH MT (3 cell lines) and IDH WT(2 cell lines) treated with VPA (A), Panobinistat (B), and Belinostat (C) for 1 week. D-E Dose response curve of mIDH1MT and mIDH1WT treated with VPA (D) or Belinostat(E) for 5days. F. D-2HG content in the MT cell lines G Kaplan-Meier survival curve for mice treated with either saline or VPA (300mg/kg, twice daily) implanted with BT142 ****P value< 0.0001. G Kaplan-Meier survival curve for mice with NPAC54B or NPAIC1 xenograft treated with either saline or VPA (300mg/kg, twice daily) ***P value<0.001.

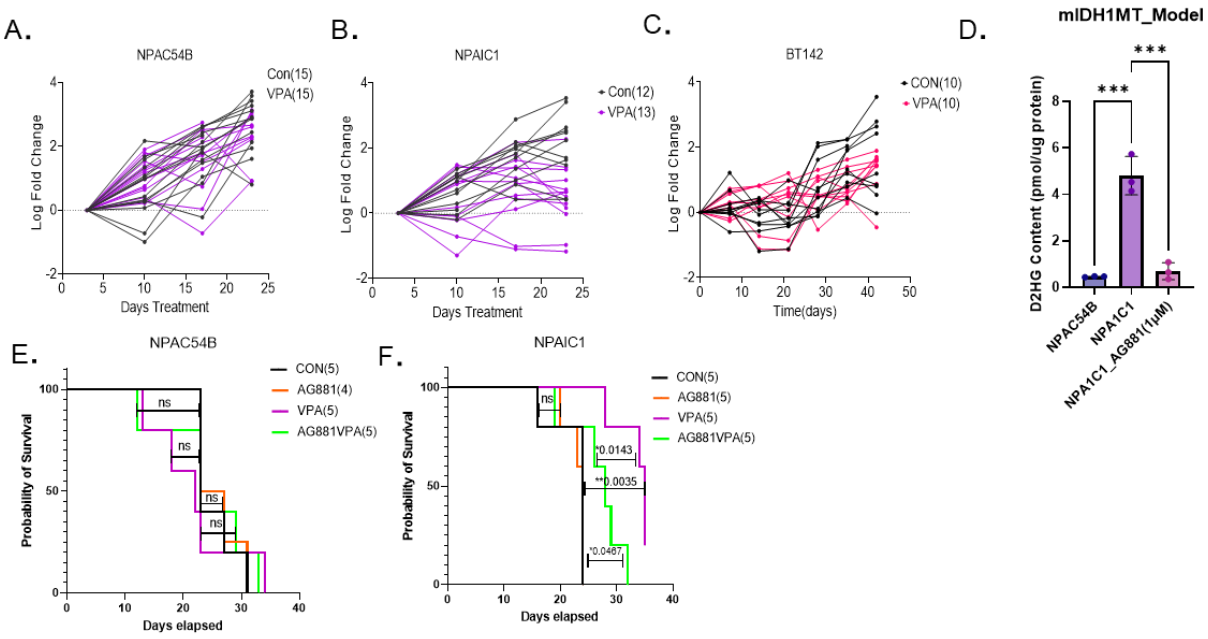

Supplementary Fig1: VPA slows down tumor growth in vivo

A-B In vivo tumor progression of NPAC54B and NPAIC1 xenograft in mice treated with either saline or VPA (300mg/kg, twice daily). C In vivo tumor progression of BT142 xenograft in mice treated with either saline or VPA (300mg/kg, twice daily). D D2HG measurement in mIDH1MT model E-F Kaplan-Meier survival curve for mice with NPAC54B or NPAIC1 xenograft treated with either saline, VPA (300mg/kg, twice daily), AG881(2mg/kg, twice daily) or both. **P value<0.01; *P value<0.05

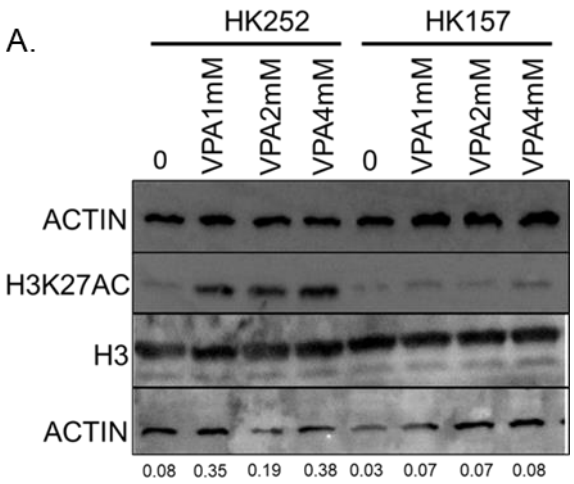

Supplementary Fig2: VPA increases H3K27ac in IDH MT glioma cell line HK252

A. Representative western blot showing H3K27ac in HK252 and HK 157 after 4 days of treatment with VPA 1mM, 2mM & 4mM

VPA upregulates genes associated with neurogenesis and inhibits lipid metabolic processes primarily in IDH MT glioma

VPA is a multifaceted drug that has several direct[75] and indirect targets[76]. Given the pleiotropic effects of VPA we wanted to understand why IDH MT glioma cell lines were particularly sensitive to VPA. Given that HDACs are a primary target of VPA, we treated a IDH MT cell line HK252 and a IDH WT cell line HK157 with increasing concentration of VPA for 4 days and looked at histone 3 lysine 27 acetylation(H3K27ac), a histone mark associated with active transcription and enhancer. Consistent with the function of VPA as a HDACi, VPA increased H3K27ac in IDH MT cell line HK252 (supplementary Fig2). Semi quantitative analysis of the western blot (WB) suggested in HK252 the increase in H3K27ac was 4.5 times greater than control whereas in HK157 the increase in H3K27ac was 2.5 times greater than the control. This suggests VPA may have a larger transcriptomic effect in HK252 than HK157.

We next treated multiple IDH MT glioma cell lines (HK252, HK213, BT142, MGG119) and IDH WT glioma cell lines (HK157, HK408, HK393, HK206 & HK350) with 1mM VPA for 48 hours and conducted bulk RNA sequencing to get a better understanding of the transcriptomic effect of VPA. A greater number of genes were upregulated than downregulated with VPA treatment in both IDH WT and IDH MT glioma cell lines. How many genes went up versus down seemed to be cell line dependent and no clear transcriptomic pattern distinguished IDH MT from IDH WT (supplementary Fig3). Interestingly, HK252, which showed higher increase in H3K27ac compared to HK157 also had twice the number of genes upregulated compared to HK157 suggesting there may be a correlation between the magnitude of increase in H3K27ac and transcription.

To better understand what biological processes are altered by VPA we performed gene set enrichment analysis (GSEA) and compared what gene ontology (GO) terms were upregulated versus downregulated with VPA treatment in WT versus MT cell lines. We found in both the primary glioma cell lines (Fig2A) and the syngeneic mIDH1 glioma model (Fig2C) GO terms related to cell cycle and DNA repair were downregulated whereas GO terms related to neuronal differentiation and neurogenesis were upregulated after VPA treatment. In the primary MT glioma cell lines neurogenic genes such as (BCL11B, ITGA5, STMN2 and BDNF) had a higher increase in gene expression compared to IDH WT after VPA treatment. In the mIDH1 glioma cell VPA increased *Bdnf* expression in the mIDH1MT cell line but inhibited *Bdnf* expression in the mIDH1WT cell line. VPA also increased ion channel genes such as (KCNA1, KCNA4, SCN9A) and TMEM119, a gene commonly associated with microglia, both in mIDH1 and primary IDH MT cell lines. Interestingly, glial genes such as (GFAP, HEPACAM) were downregulated more in the IDH MT cell lines compared to IDH WT cell lines after VPA treatment in both IDH MT models. In addition, VPA upregulated DEPTOR, a negative regulator of mTOR much more in the IDH MT cell lines than IDH WT. This suggests perhaps VPA treatment influences the mTOR pathway in IDH MT glioma. Finally, VPA downregulated MKI67, and cell cycle genes such as PLK1, PLK4, BUB1,

and AURKA but the effect on cell cycle genes were stronger in the IDH WT cell lines compared to IDH MT.

Nonetheless, the normalized enrichment score (NES) for neurogenesis and cell cycle related terms were not very different between IDH WT and IDH MT so we instead asked what biological processes were only altered in IDH MT and not in IDH WT. GO terms related to epithelial and osteoblast differentiation, and immune system (Fig2B) were upregulated only in the primary MT cell lines but not in the IDH WT. In the mIDH1 glioma model GO terms related to cellular stress and hormone mediated signaling (Fig2D) were upregulated only in the mIDH1MT and not mIDH1WT. In both primary MT cell lines and mIDH1 MT cell line GO terms related to lipid and sterol biosynthetic processes were downregulated but no change was seen in the respective WT cell lines. We looked through a panel of lipogenic genes and found SREBF1, ACLY, FASN, SCD, & HMGCR were significantly downregulated in primary IDH MT cell lines after VPA treatment (Fig2E). In the syngeneic mouse model VPA only significantly downregulated mRNA expression of *Fasn* in NPAC1 cell line but not in the NPAC54B cell line (Fig2F). To sum up, short term treatment with VPA alters many genes, some of which are shared between WT and MT cell lines. However, we see a much robust down regulation of lipogenic genes in the primary MT glioma cell lines compared to primary IDH WT cell lines.

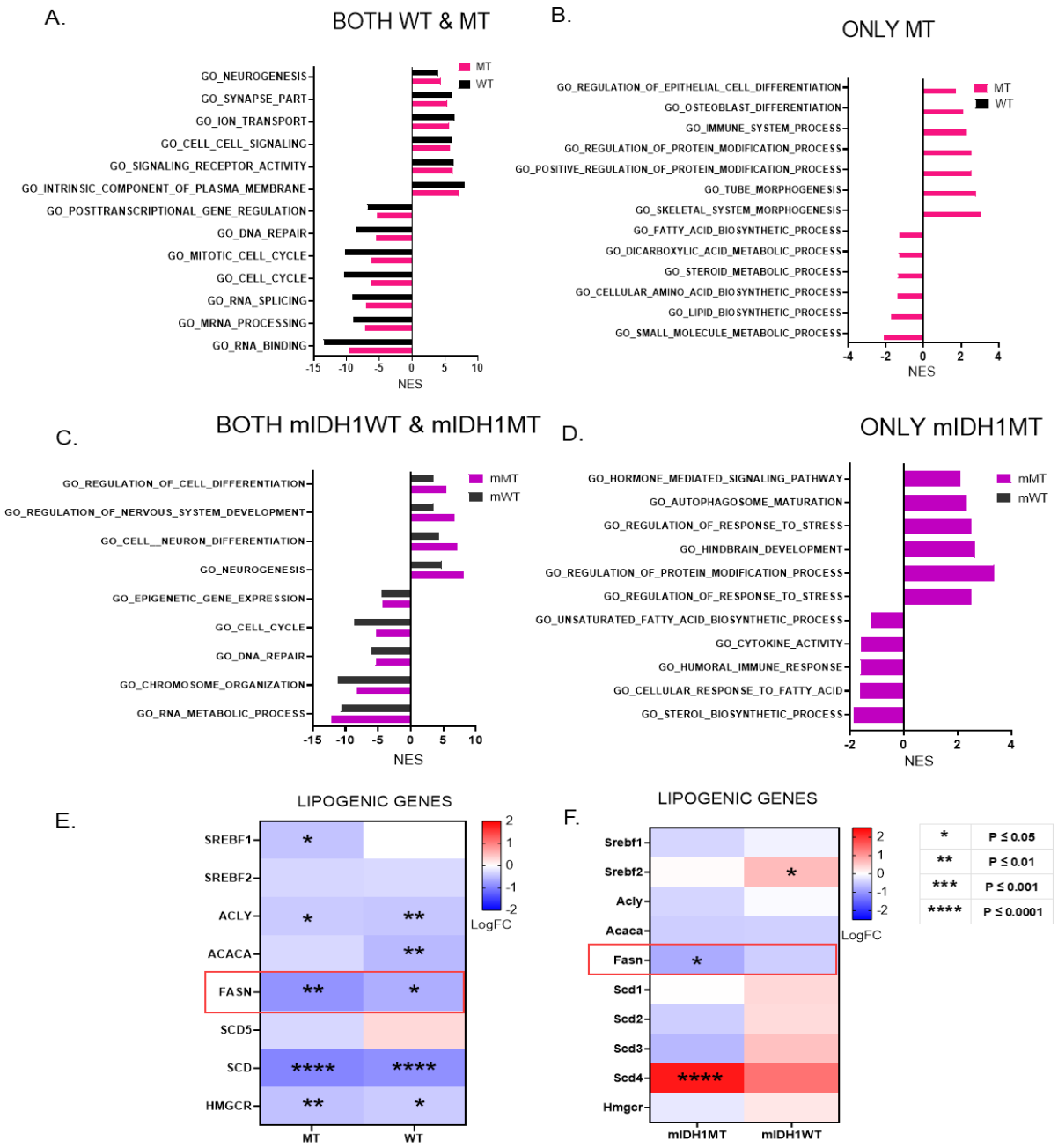
A.
BOTH WT & MT
MT
WT
GO_NEUROGENESIS
GO_SYNAPSE_PART
GO_ION_TRANSPORT
GO_CELL_CELL_SIGNALING
GO_SIGNALING_RECEPTOR_ACTIVITY
GO_INTRINSIC_COMPONENT_OF_PLASMA_MEMBRANE
GO_POSTTRANSCRIPTIONAL_GENE_REGULATION
GO_DNA_REPAIR
GO_MITOTIC_CELL_CYCLE
GO_CELL_CYCLE
GO_RNA_SPLICING
GO_MRNA_PROCESSING
GO_RNA_BINDING
-15 -10 -5 0 5 10
NES
B.
ONLY MT
MT
WT
GO_REGULATION_OF_EPITHELIAL_CELL_DIFFERENTIATION
GO_OSTEOBLAST_DIFFERENTIATION
GO_IMMUNE_SYSTEM_PROCESS
GO_REGULATION_OF_PROTEIN_MODIFICATION_PROCESS
GO_POSITIVE_REGULATION_OF_PROTEIN_MODIFICATION_PROCESS
GO_TUBE_MORPHOGENESIS
GO_SKELETAL_SYSTEM_MORPHOGENESIS
GO_FATTY_ACID_BIOSYNTHETIC_PROCESS
GO_DICARBOXYLIC_ACID_METABOLIC_PROCESS
GO_STEROID_METABOLIC_PROCESS
GO_CELLULAR_AMINO_ACID_BIOSYNTHETIC_PROCESS
GO_LIPID_BIOSYNTHETIC_PROCESS
GO_SMALL_MOLECULE_METABOLIC_PROCESS
-4 -2 0 2 4
NES
C.
BOTH mIDH1WT & mIDH1MT
mMT
mWT
GO_REGULATION_OF_CELL_DIFFERENTIATION
GO_REGULATION_OF_NERVOUS_SYSTEM_DEVELOPMENT
GO_CELL__NEURON_DIFFERENTIATION
GO_NEUROGENESIS
GO_EPIGENETIC_GENE_EXPRESSION
GO_CELL_CYCLE
GO_DNA_REPAIR
GO_CHROMOSOME_ORGANIZATION
GO_RNA_METABOLIC_PROCESS
-15 -10 -5 0 5 10
NES
D.
ONLY mIDH1MT
mMT
mWT
GO_HORMONE_MEDIATED_SIGNALING_PATHWAY
GO_AUTOPHAGOSOME_MATURATION
GO_REGULATION_OF_RESPONSE_TO_STRESS
GO_HINDBRAIN_DEVELOPMENT
GO_REGULATION_OF_PROTEIN_MODIFICATION_PROCESS
GO_REGULATION_OF_RESPONSE_TO_STRESS
GO_UNSATURATED_FATTY_ACID_BIOSYNTHETIC_PROCESS
GO_CYTOKINE_ACTIVITY
GO_HUMORAL_IMMUNE_RESPONSE
GO_CELLULAR_RESPONSE_TO_FATTY_ACID
GO_STEROL_BIOSYNTHETIC_PROCESS
-2 0 2 4
NES
E.
LIPOGENIC GENES
SREBF1
SREBF2
ACLY
ACACA
FASN
SCD5
SCD
HMGCR
MT
WT
2
1
0
-1
-2
LogFC
F.
LIPOGENIC GENES
Srebf1
Srebf2
Acly
Acaca
Fasn
Scd1
Scd2
Scd3
Scd4
Hmgcr
mIDH1MT
mIDH1WT
2
1
0
-1
-2
LogFC
* P ≤ 0.05
** P ≤ 0.01
*** P ≤ 0.001
**** P ≤ 0.0001

Fig2: VPA inhibits lipid metabolic processes only in IDH MT GBM

A,C. GSEA analysis showing top gene ontology terms upregulated and downregulated in both primary WT and MT cells lines (A) mIDH1WT and mIDH1MT cell lines(C).Only upregulated and downregulated in primary MT cell lines (B) and mIDH1WT and mIDH1MT cell lines (D). E-F Heatmap of differentially expressed lipogenic genes in primary WT and MT cell lines (E) and mIDH1WT and mIDH1MT cell lines (F)

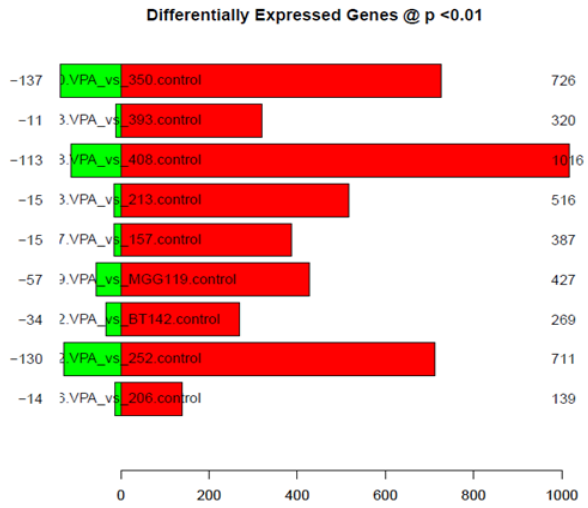

Supplementary Fig3: A greater number of genes are upregulated by VPA in both IDH MT and WT cell lines

A. Results of contrast analysis in Edge R (p <0.01). Red shows the total number of genes upregulated by VPA and green shows the total number of genes downregulated by VPA

Treatment with VPA alters promoter chromatin accessibility of multiple lipogenic genes

Given that we saw a major upregulation of genes by RNA seq we next wanted to assess the impact of VPA on overall chromatin accessibility in IDH MT cells. We hypothesized with VPA treatment we would see chromatin decondensation. We analyzed ATAC and RNA seq data from a recent study[21] that treated two IDH WT (HK357, HK350) and IDH MT primary cell lines (HK252, HK211 & BT142) with VPA(1mM) and SAHA (100nM) for 5 days. We report new analysis of the data that the study did not report or discuss. The overall chromatin accessibility across different chromatin regions did not change with 5 days of treatment with either VPA or SAHA. In HK357 and BT142 overall chromatin accessibility decreased with treatment with VPA but not SAHA (Supplementary Fig4A). We integrated RNA and ATAC seq data sets and asked whether genes upregulated by VPA have greater promoter accessibility. In the IDH WT cell lines not much change was seen across promoters of upregulated (Supplementary Fig4B) or downregulated (Supplementary Fig4C) genes after VPA treatment. In the IDH MT glioma cell lines there was not much change in promoter chromatin accessibility for upregulated genes but in the VPA downregulated genes we saw a decrease in promoter chromatin accessibility (Supplementary Fig4E). In depth analysis showed there was a significant decrease in promoter chromatin accessibility with VPA treatment across multiple lipogenic genes (ACACA, FASN, SCD & HMGCR) only in the IDH MT but not IDH WT cell lines (Supplementary Fig4F).

Similar to what we see in patient tissues our IDH MT cell lines are more methylated than IDH WT cell lines[21] so we wondered whether a longer treatment with VPA would be necessary to increase chromatin accessibility in MT cell lines. We treated HK252 and HK211 with VPA longer term for three weeks, conducted ATAC and RNA seq, and compared the results to our above findings. Treatment with VPA for three weeks decreased overall chromatin accessibility in HK252

and HK211 (Supplementary Fig3D). We again integrated ATAC and RNA seq data and in HK252 we saw across all genes regulated by VPA the average ATAC signal decreased (Fig3A). In the VPA upregulated genes in HK252 no change was seen at TSS (0) but 1000bp upstream of the TSS showed some open regions (Fig3B). In HK211 not much change was seen at the TSS of the VPA upregulated genes (Supplementary Fig3A). Similar to what we saw with the short term VPA treatment, long term VPA treatment decreased promoter accessibility of VPA downregulated genes in HK252(Fig3C) and HK211 (Supplementary Fig3B). We also compared gene expression changes of VPA with short term (48hr treatment) and long term (3 weeks) in HK252. Both short and long term VPA treatment upregulated more genes and downregulated a small number of genes. 890/1308 (68%) of the short term VPA upregulated genes (Fig3D) were also up after long term treatment. 80/272 (30%) of the short term VPA downregulated genes (Fig3E) were also down after long term treatment. Long term treatment with VPA showed decrease in chromatin accessibility at promoters of FASN, SCD, and HMGCR (Fig3F) like what we saw in the short-term treatment (Fig3G). GSEA enrichment analysis showed mTOR signaling, along with fatty acid metabolism, and pathways related to cell cycle and DNA repair were down and inflammatory response was up after long term treatment of HK252 with VPA (Fig3I). Interestingly, long term VPA treatment increased GFAP expression in HK252 but not in HK211 suggesting long term VPA treatment may induce differentiation in some IDH MT glioma cell lines and not others. Long term treatment in HK211 did not increase GFAP expression. Motif analysis identified several interesting transcription factor motifs after VPA treatment. Although we noticed there was variability in motif enrichment across cell lines. Motifs for IRF4, NYFA, NFYB, ATF4 and DDIT3 (Fig3G) were enriched in HK252 after long term VPA treatment. In HK211 long term treatment showed enrichment for IRF4 and ATF2 but short term showed enrichment for NFYA. In BT142 short term treatment showed enrichment for IRF4. The trimeric transcription factor NF-Y formed by NF-YA, NF-YB and NF-YC can bind to promoter of lipogenic genes and regulate de novo lipid metabolism

genes in cancer cells[77]. ATF4, ATF2, and DDIT3 on the other hand are closely associated with endoplasmic reticulum stress pathways. Some of these transcription factors may be important targets for IDH MT glioma but since there was variability across cell lines, we focused on the lipogenic genes that were consistently downregulated with VPA treatment in MT cell lines.

Together our short- and long-term RNA and ATAC seq data strongly suggested that VPA alters lipid metabolism in IDH MT glioma. We identified several lipogenic candidates through which VPA may be acting. mTOR plays a role in lipid metabolism and our RNA and ATAC seq data suggested that VPA may inhibit the mTOR pathway. The mTOR pathway has been identified by several studies to regulate FASN (Fig4A)[78,79] hence we decided to further focus on the mTOR pathway and FASN regulation by VPA.

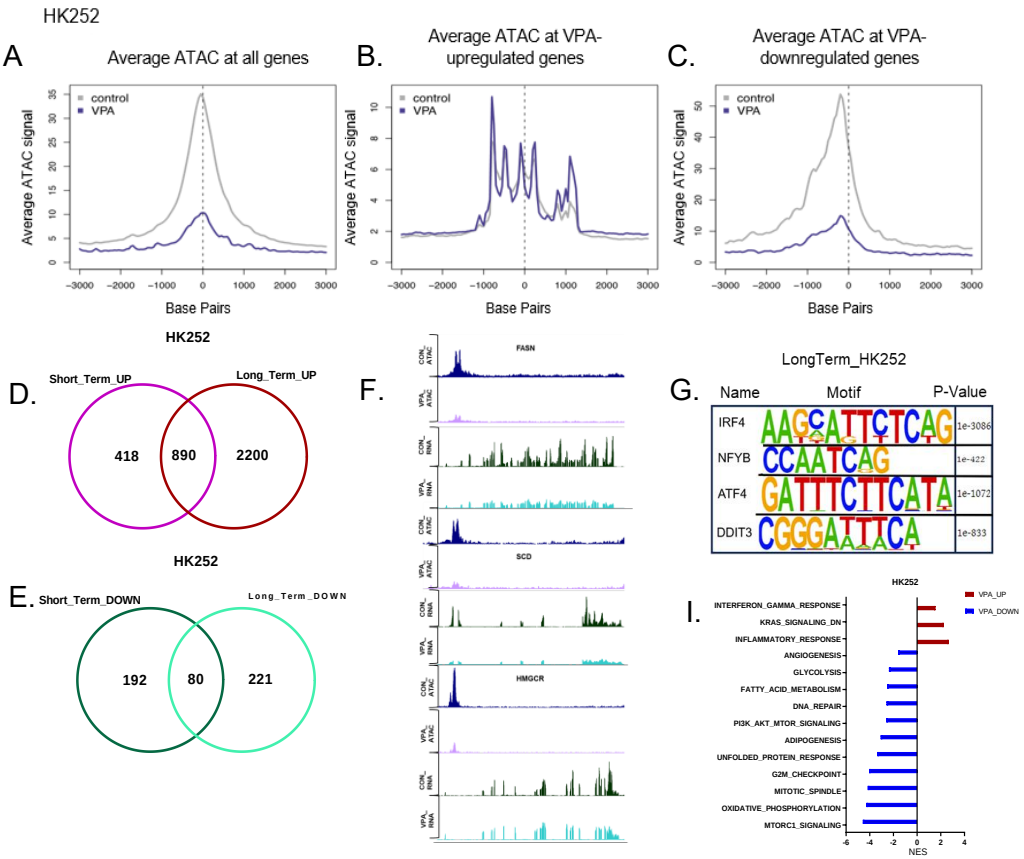

Fig3: Long term treatment with VPA decreases overall chromatin accessibility and reveals TF motif enrichment associated with lipid metabolism and ER stress in IDH MT cell line HK252. A-C HK252 was treated with VPA 1mM for 3 week and ATAC and RNA seq data was integrated to map chromatin accessibility at genes upregulated and downregulated by VPA. (A) Shows chromatin accessibility at all genes differentially altered by VPA compared to CON. (B) Shows chromatin accessibility at genes upregulated by VPA (C) Shows chromatin accessibility at genes downregulated by VPA, Transcription start site, TSS=0. D. Venn diagram showing upregulated gene overlap in HK252 after short term(48h) and long term(3weeks) treatment with VPA. E. Venn diagram showing downregulated gene overlap in HK252 after short term(48h) and long term(3weeks) treatment with VPA. E. Genome browser track for ATAC seq for FASN after 3 weeks treatment with VPA 1mM. F. Genome browser track for ATAC & RNA seq for FASN, SCD & HMGCR after 3 weeks treatment with VPA 1mM. H. Selected TF identified by Homer Motif Analysis in VPA treated Hk252. I GSEA VPAvsCON hallmark pathways in HK252 treated for 3 weeks.

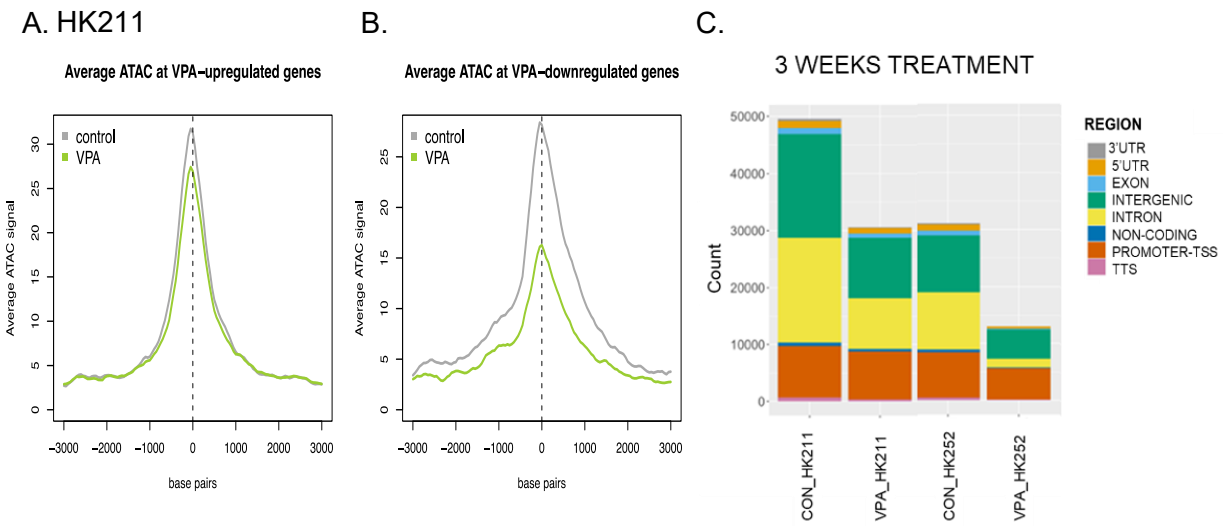

Supplementary Fig4: VPA treatment also decreases chromatin accessibility in HK211 cell line A-C HK211 was treated with VPA 1mM for 3 week and ATAC and RNA seq data was integrated to map chromatin accessibility at genes upregulated and downregulated by VPA. (A) Shows chromatin accessibility at all genes differentially altered by VPA compared to CON. (B) Shows chromatin accessibility at genes upregulated by VPA (C) Shows chromatin accessibility at genes downregulated by VPA, Transcription start site, TSS=0. D. Shows proportion of ATAC peaks at different chromatin region

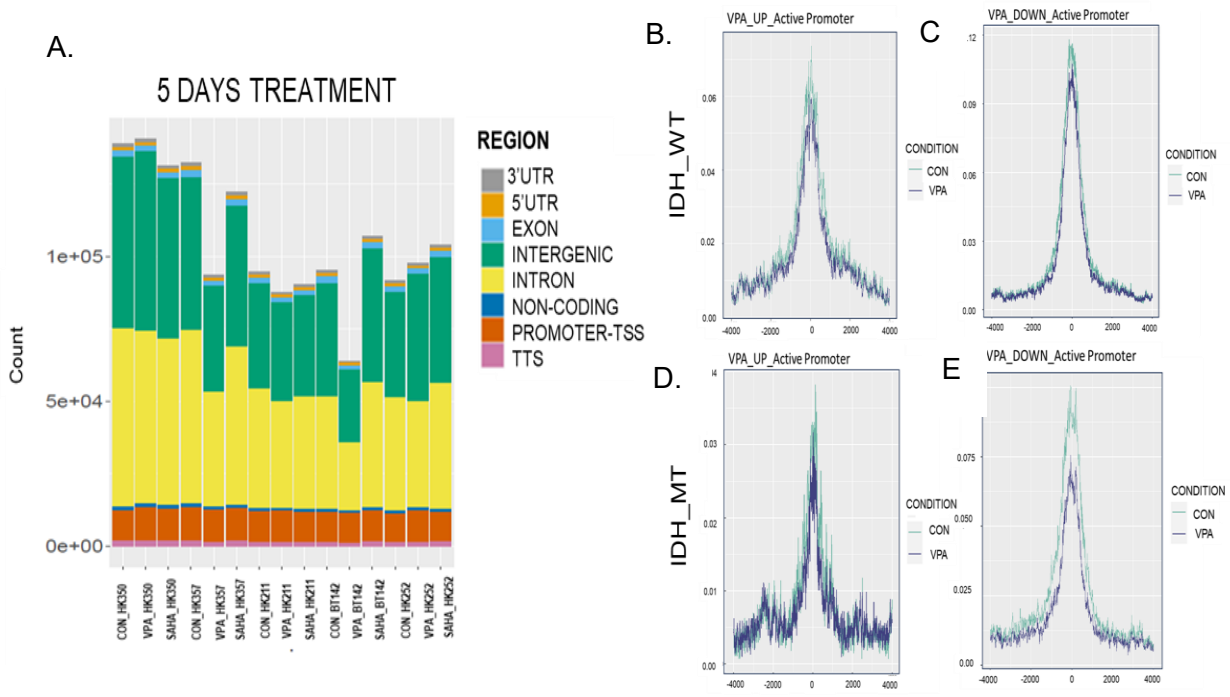

F.

Gene Name	logFC_WT_VPA_vs_WT_CON	logFC_WT_SAHA_vs_WT_CON	logFC_IDH1m_VPA_vs_IDH1m_Control	logFC_IDH1m_SAHA_vs_IDH1m_CON	PValue_WT_VPA_vs_WT_Control	PValue_WT_SAHA_vs_WT_CON	PValue_IDH1m_VPA_vs_IDH1m_CON	PValue_IDH1m_SAHA_vs_IDH1m_CON
FASN	-0.071003572	0.257584	-0.37907	-0.21694	0.71441	0.183056	0.018034	0.174006
SCD	-0.175927157	0.061432	-0.42899	-0.23081	0.273152	0.703005	0.001163	0.075885
HMGCR	-0.112348906	0.255764	-0.32061	-0.16233	0.47186	0.101332	0.012256	0.2021
ACACA	-0.417270724	0.272683	-0.87299	-0.20815	0.059314	0.206044	3.7E-05	0.284959
SREBF1	-0.06779479	0.266701	-0.52354	-0.17793	0.763612	0.233732	0.012467	0.383316

Supplementary Fig5: Short term VPA treatment decreases promoter chromatin accessibility across multiple lipogenic genes only in MT but not WT cell lines. A. Shows proportion of ATAC peaks at different chromatin region with 5 days of VPA (1mM) and SAHA (100nM) treatment B. chromHMM annotation of active ATAC peaks for genes upregulated and downregulated by VPA, B-C (IDHWT) D-E (IDHMT) respectively. F. DEA Edge R analysis of differential ATAC seq peaks for FASN gene C. DEA Edge R analysis of differential ATAC seq peaks for lipogenic genes.

VPA inhibits mTOR pathway and downregulates FASN protein expression

To understand whether VPA had any effect on the mTOR pathway and whether mTOR had any role in regulating FASN protein expression in IDH MT glioma we treated 2 of our IDH MT glioma cell lines HK252 and BT142 with VPA for four days and looked at phosphorylation of ribosomal protein S6 (PS6) and FASN protein expression. VPA decreased phosphorylation of S6 and FASN protein expression in both HK252 (Fig4C) and BT142(Fig4D). In HK157 a small decrease in PS6 was seen with 1mM concentration of VPA but semiquantitative analysis of the western blot (WB) showed no change in PS6 with higher concentration of VPA in HK157(Fig4B). We also treated HK252 with rapamycin (RAPA) and saw a decrease in PS6 and FASN protein expression (Fig4E). Treatment with RAPA and RAPA with VPA showed a similar decrease in FASN protein expression in HK252(Fig 4F). To further test that mTOR pathway is involved in regulation of FASN, we knocked down PTEN in a IDH WT glioma cell line (HK157) that has WT PTEN and no PTEN CNV loss. Knock down of PTEN in HK157 increased both PAKT, PS6, and FASN protein expression (Fig4E). Together this suggests mTOR pathway is involved in regulation of FASN protein expression. We then treated HK157, HK252, & BT142 with VPA, RAPA, and the combination of both drugs. We wondered whether inhibition of mTOR would rescue some of the inhibitory effect of VPA. Both VPA and RAPA inhibited growth of the primary WT and the MT cell lines. In the HK252 cell line there was no significant difference in growth between VPA and VPA+RAPA (Fig4G) condition suggesting both drugs may work through similar pathway. However, HK157 and BT142 were both more sensitive to RAPA (100nM) than HK252. Combination of VPA+RAPA was better at inhibiting growth of these two cell lines than VPA alone. However, there was no significant difference in growth between RAPA and RAPA+VPA in these two cell lines (Fig4G). Interestingly, only the mIDH1MT cell line NPAIC1 responded to RAPA treatment but not the mIDH1WT cell line NPAC54B (Supplementary Fig6B). Treatment with VPA only decreased PS6 in NPAIC1 but not in NPAC54B (Supplementary Fig6A). However, we saw a decrease in

FASN protein expression in both NPAC54B and NPAIC1 (Supplementary Fig6A). In addition, compared to VPA alone combination of VPA+RAPA was better at inhibiting growth of NPAC54B but there was no significant difference in growth inhibition between VPA and VPA+RAPA in NPAIC1(Supplementary Fig6C). This suggests the mIDH1MT is more sensitive to mTOR inhibition than mIDH1WT.

Together, we conclude at least some part of VPA's growth inhibitory effect is due to mTOR inhibition at least in the MT cell line HK252 and mIDH1MT model and that the mTOR pathway is involved in regulation of FASN protein expression.

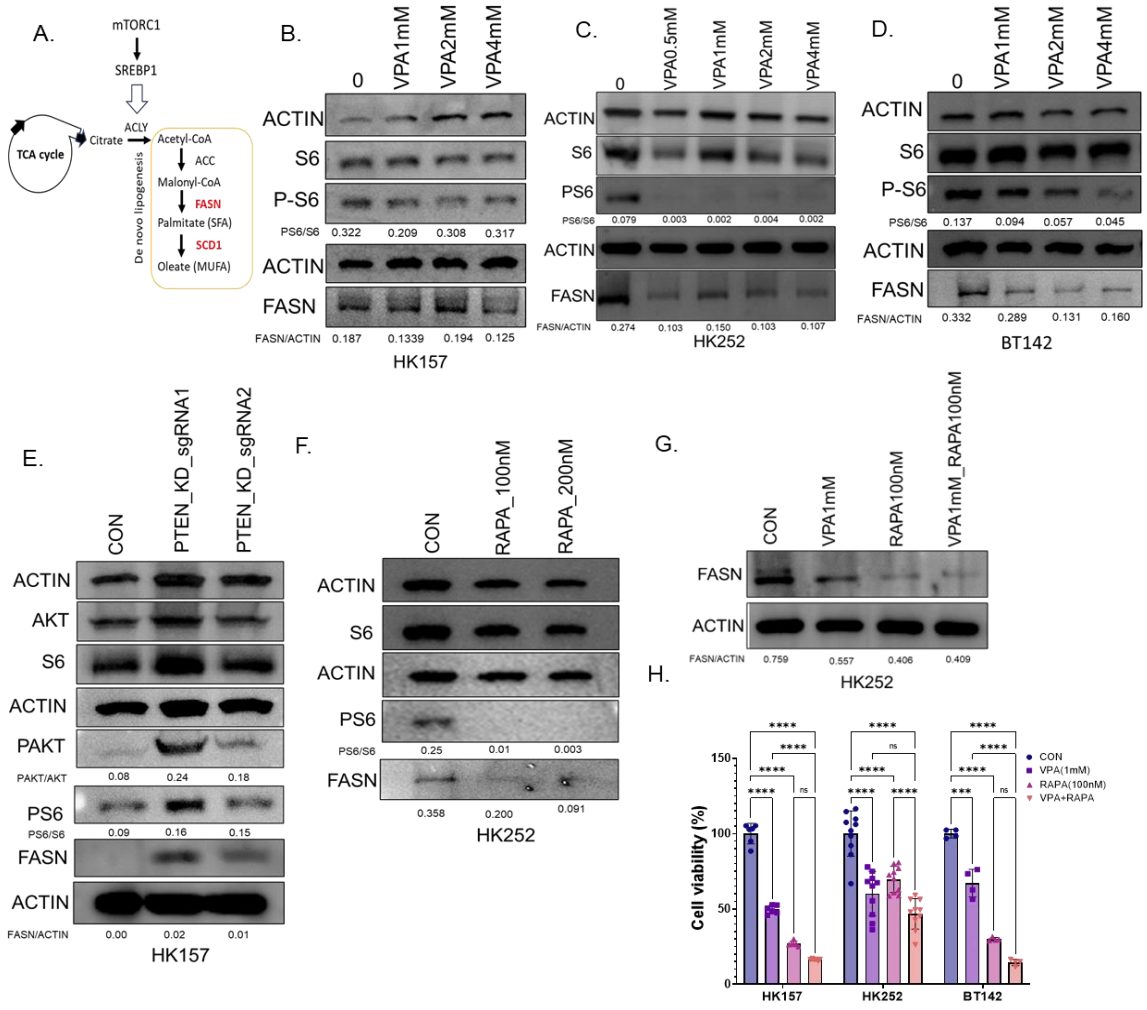

Fig4: VPA treatment decreases PS6 and FASN protein expression

A. Schematic of mTORC1 regulation of lipogenic genes via activation of SREBP1

B-D Representative western blots of IDHWT GBM HK157 (B)IDH MT GBM HK252 (C) BT142 (D) treated with different doses of VPA for 4 days.

E Representative western blot of IDH WT cell line HK157 after PTEN CRISPR knockdown.

F Representative western blot of MT cell line HK252 treated with RAPA for 4days.

G. Representative western blot of MT cell line HK252 treated with VPA, RAPA, & combination for 4days.

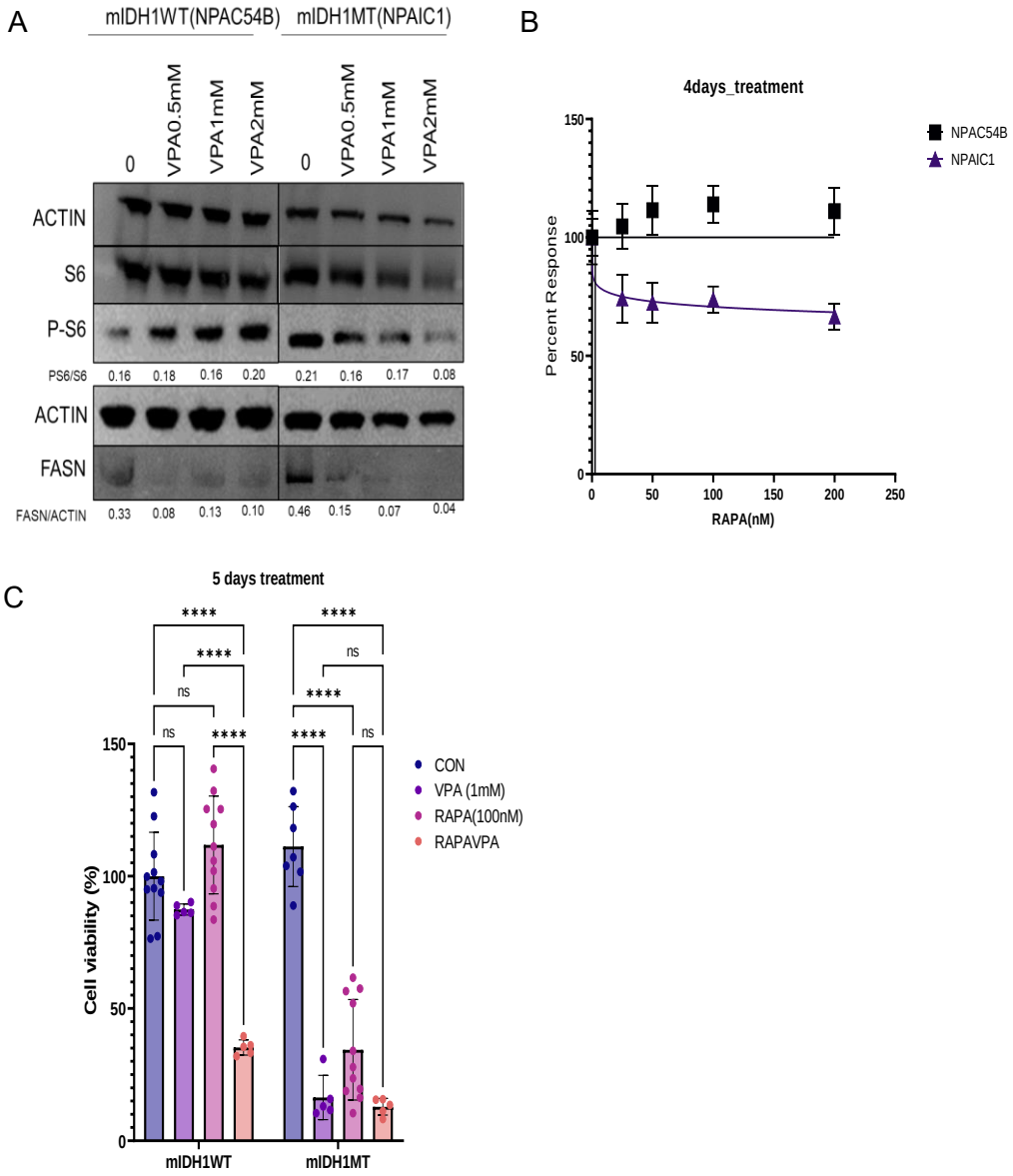

Supplementary Fig6: mIDH1MT (NPAIC1) cell line is more sensitive to RAPA than mIDHWT (NPAC54B)

A. Representative western blot of mIDH1MT and mIDHWT showing PS6 and FASN

B. Dose response curve for NPAIC1 and NPAC54B treated with RAPA for 4 days

C. Growth inhibitory response of NPAIC1 and NPAC54B to VPA, RAPA and the combination of both drugs. 2-way ANOVA *P value<0.0001; Error bars ±SD.

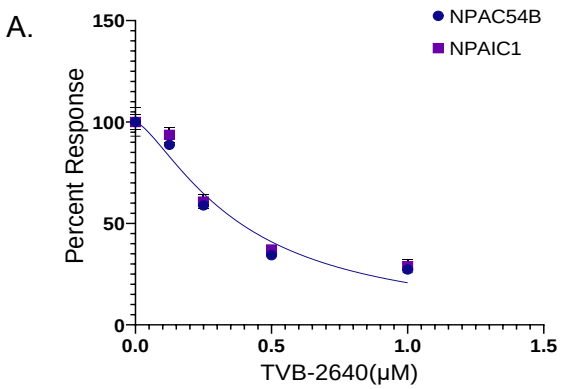

Supplementary Fig7: Both NPAIC1 and NPAC54B respond to TVB-2640.

Dose response curve for NPAIC1 and NPAC54B treated with TVB-2640

IDH MT glioma are sensitive to selective FASN inhibitor TVB-2640 and FASN inhibition regulates cell cycle genes.

We next wanted to ask whether inhibiting FASN directly would have any effect on growth of IDH MT glioma. We tested a selective reversible FASN inhibitor TVB-2640 in two 2 IDH WT and 2 IDH MT glioma cell lines (Fig5A). The IDH MT cell lines tested were more sensitive to TVB-2640 compared to the two IDH WT cell lines tested (Fig5D). IDH WT cell line HK217 did not respond to TVB-2640 (Fig5C). IDH WT cell line HK157 (Fig5B) and IDH MT cell lines HK252 (Fig5E) and BT142(5F) did respond to TVB-2640. The MT cell lines had lower IC50 for TVB-2640 HK252(IC50, .0084), BT142(IC50, 1.065e-005) compared to WT cell line HK157(IC50, 0.54). Supplementation of palmitate in the regular GBM media rescued growth inhibitory effect of TVB-2640 in HK157, HK252 & BT142. HK252 was most sensitive to both TVB-2640 and palmitate treatment (Fig5E). Both mIDHMT cell lines NPAC54B and NPAIC1 were sensitive to TVB-2640 (Supplementary Fig7).

Next, we knocked down FASN in HK252 and BT142 (Fig5G). FASN knockdown inhibited growth of both HK252 and BT142. After FASN knockdown it was difficult to grow HK252 even with

palmitate supplementation in the media. In BT142 palmitate could rescue growth inhibitory of FASN shRNA1 and shRNA3 but not shRNA2 (data not shown). Palmitate could rescue almost 90% of the effect of FASN knockdown with shRNA1 (Fig5J) in BT142. Hence, FASN KD with shRNA1 was used for additional experiments.

To understand what genes are regulated by FASN inhibition we treated HK252 and BT142 with TVB-2640, palmitate, and TVB-2640 with palmitate and conducted RNA sequencing. In both HK252 and BT142 TVB-2640 inhibited genes involved in cell cycle (Supplementary Fig8A) which could be rescued by palmitate supplementation in BT142 but only partially in HK252. In HK252 and BT142 treatment with TVB-2640 inhibited DNA repair and cell cycle (Supplementary Fig8A, B). In HK252 perk mediated unfolded protein response (UPR) and stress fiber assembly was upregulated (Supplementary Fig8B) whereas in BT142 multiple biological processes related to cholesterol metabolism were upregulated (Supplementary Fig8C) suggesting potential compensatory mechanism. We next wanted to know if VPA altered some of the same genes as TVB-2640. We compared both up and downregulated genes and identified a suite of 128 genes downregulated by both VPA and TVB-2640 (Supplementary Fig8D). We performed reactome pathway analysis on the common genes and found that most of them were involved in regulation of cell cycle (Supplementary Fig8E). Interestingly, In HK252 and BT142 TVB-2640 and FASN knockdown in BT142 increased mRNA expression of HMGCR (Supplementary Fig8F) a key enzyme involved in cholesterol biosynthesis but VPA treatment inhibited mRNA expression of HMGCR (Supplementary Fig8G). In summary, we found that IDH MT are vulnerable to FASN inhibition and VPA and FASN converges on regulation of cell cycle genes.

However, we were most interested understanding the effect of these drugs on the lipidome.

Free fatty acids can induce UPR and lipotoxicity[80] and increased unfolded protein response and ER stress in the HK252 cell line suggested free fatty acids might be altered after FASN

inhibition. Cancer cells often form lipid droplets to reduce excess free fatty acids so next we investigated how VPA and TVB-2640 alter free fatty acid and lipid droplet composition in MT and WT cell lines.

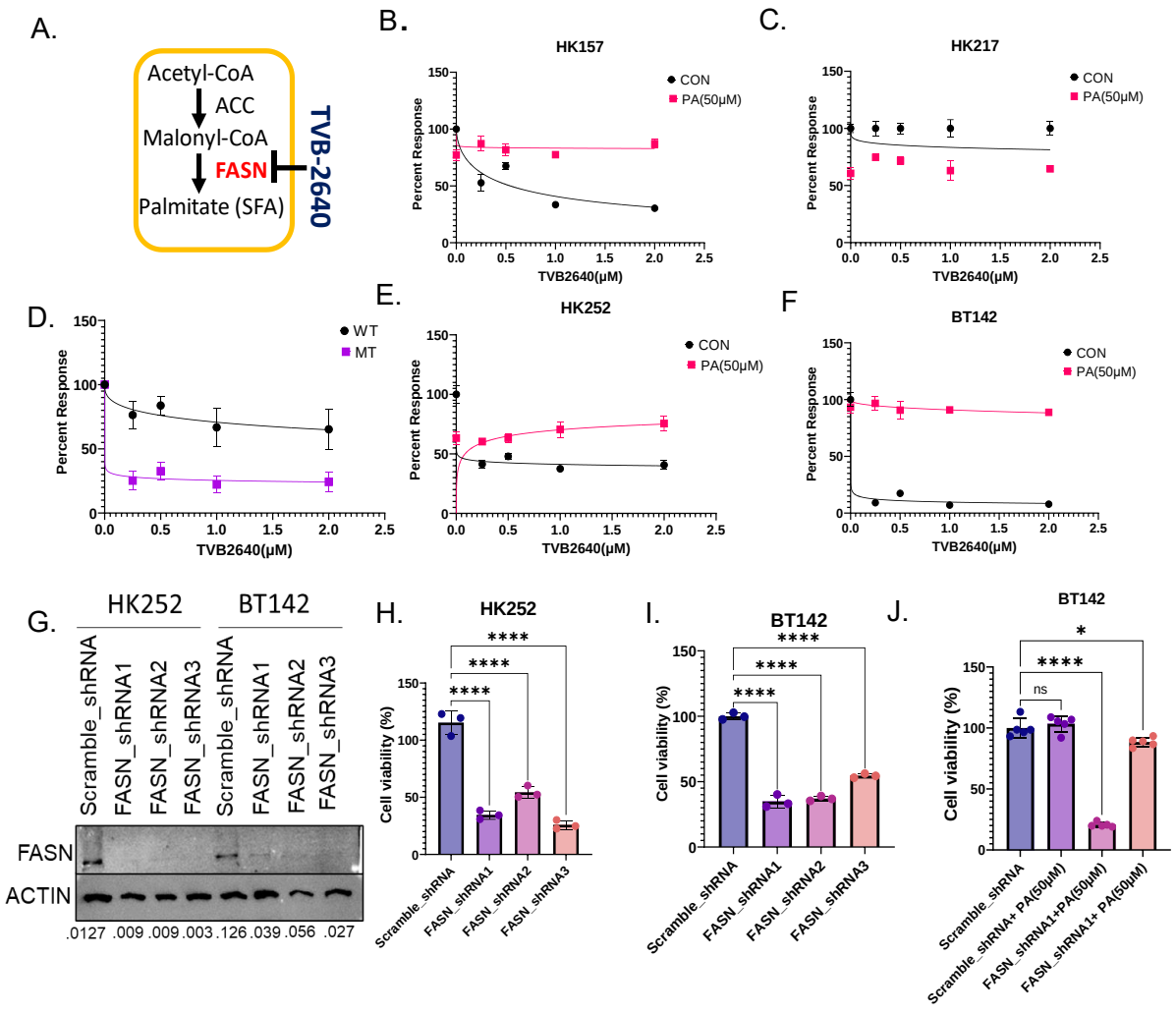

Fig5: FASN inhibitor TVB-2640 and FASN knockdown inhibits growth of IDH MT GBM and can be rescued by palmitate.

A. Schematic of TVB-2640 inhibiting FASN

B-C, E-F Relative percent growth of WT and MT cell lines to TVB-2640, HK157(B), HK217(C), HK252(E), BT142(F) with and without palmitate

D. Dose response curve of TVB-2640 comparing WT and MT

G. Western blot of FASN knockdown

H-I Relative percent growth of HK252 (D) and BT142 (E) after FASN knockdown

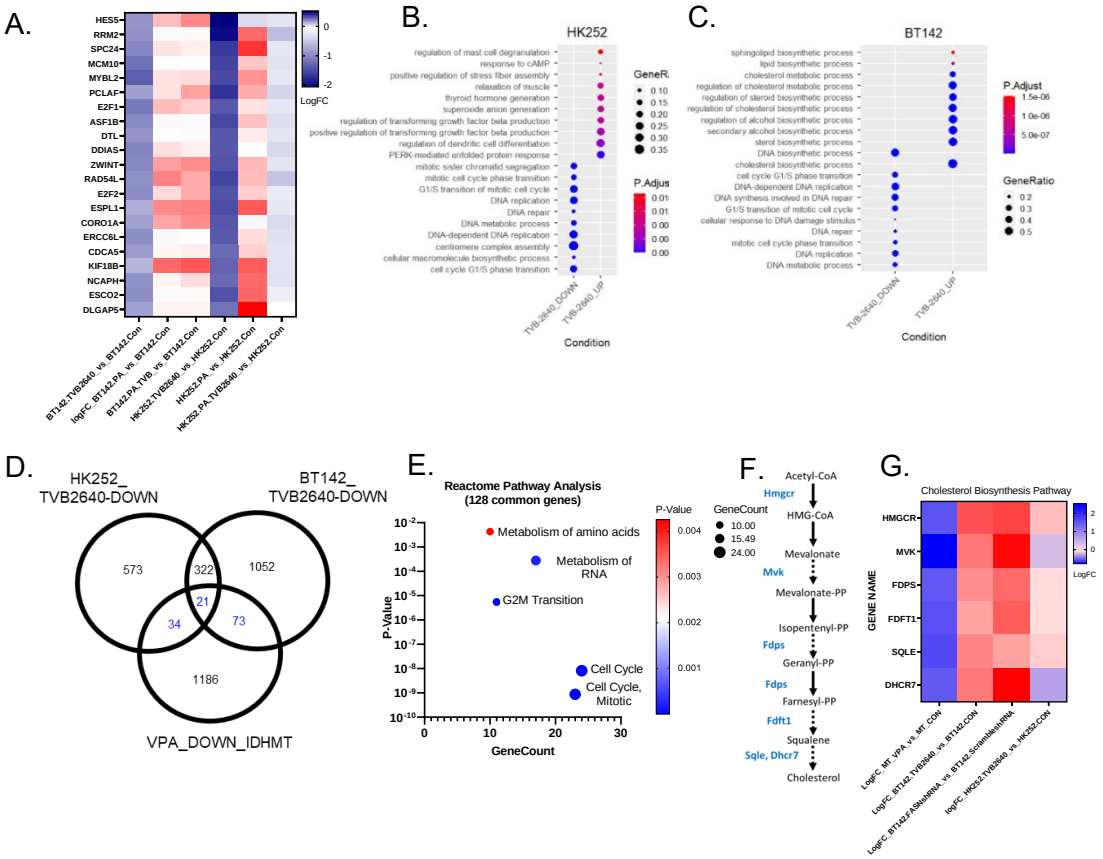

Supplementary Fig8: In IDH MT GBM, FASN inhibition via TVB-2640 and VPA converges on regulation of cell cycle genes but has opposing effect on genes regulating cholesterol biosynthesis pathway

A. Heat map showing a short list of common genes inhibited by TVB-2640 in both HK252 and BT142 B-C Dot plot showing upregulated and downregulated GO terms for MT cell lines HK252 (B) and BT142(C) after 4 days of treatment with TVB-2640(1μM). D Venn diagram showing overlap of genes downregulated by both TVB-2640 and VPA in IDH MT GBM cell lines. E. Reactome pathway analysis (DAVID) on the common genes regulated by both VPA and TVB-2640. F Cholesterol synthesis pathway G. Heatmap showing how genes in the cholesterol pathway are altered by VPA and TVB-2640

VPA and TVB-2640 alters free fatty acid and lipid droplet composition, and induces apoptosis in IDH MT glioma

Free fatty acids and apoptosis

To better understand the effect of VPA and TVB-2640 on the lipidome we treated IDH MT cell line HK252 and IDH WT cell line HK157 for 4 days with VPA and TVB-2640 and performed gas chromatography-mass spectrometry (GC-MS) and measured a panel of 33 free(non-esterified) fatty acids. In HK252 VPA significantly increased the amount of free oleic acid (18:1) (Fig6A). The ratio of free fatty acids shifted towards monounsaturated fatty acids, but the total free fatty acids did not change. TVB-2640 increased palmitic acid (16:0), stearic acid (18:0), and oleic acid (18:1) (Fig6B). However, only the increase in palmitic acid and stearic acid was statistically significant. Both the ratio of free saturated to monounsaturated free fatty acids and total free fatty acids was higher with TVB-2640 in HK252. Interestingly, in the IDH WT HK157 cell line both VPA and TVB-2640 treatment significantly decreased palmitic acid and stearic acid (Fig6C-D). Free fatty acids can trigger apoptosis[81,82] . IDH MT glioma cells were recently reported to be sensitive to oleic acid

induced apoptosis[83]. Since both VPA and TVB-2640 altered free fatty acid composition we wondered whether the drugs might be inducing apoptosis. We treated HK157 and HK252 with VPA and TVB-2640 for 4 days and stained with annexin V/7-ADD and quantified the proportion of annexin V/7-ADD positive cells using flow cytometry. We saw a significant increase in the proportion of annexin V positive cells in HK252 after 4 days of treatment with VPA and TVB-2640 (Fig6E) but not in IDH WT cell line HK157 (Fig6F). IDH MT cell line HK252 was also more sensitive to exogenous palmitic acid (Fig6G) and oleic acid (Fig6H) treatment compared to HK157. Oleic acid treatment also increased proportion of annexin V positive cells in HK252 (Fig6E) but not HK157(Fig6G). Oleic acid treatment decreased PS6 in HK252 (Supplementary Fig10A) but not in HK157 (Supplementary Fig10B) suggesting oleic acid may play a role in inhibiting the mTOR pathway. Combination of VPA and TVB-2640 did not increase the total annexin V positive cells suggesting VPA potentially triggers apoptosis via FASN.

We also knocked down FASN in BT142 and like what we saw with TVB-2640, FASN knockdown increased free fatty acids in BT142 (Supplementary Fig9A). Both palmitic and oleic acid increased after FASN knockdown but did not reach statistical significance. In BT142 we saw a significant increase in behenic acid (22:0) and arachidonic acid (20:4). We wondered whether behenic or arachidonic acid may have some lipotoxic effect in BT142. We found both HK252 and BT142 were sensitive to arachidonic acid treatment but HK157 was not (Supplementary Fig9B). BT142 was also sensitive to oleic (Supplementary Fig9C) but not palmitic acid (Supplementary Fig9D. Since BT142 already had GFP we could assess Annexin V positive cells by flow but RNA seq in BT142 with FASN knockdown showed an increase in proapoptotic genes (BAD, BAX and BOK) suggesting FASN inhibition might also induce apoptosis in BT142.

Thus far, we find that in IDH MT glioma both VPA treatment and FASN inhibition increases free fatty acids. Although different species of free fatty acids may be responsible for inducing apoptosis in HK252 versus BT142 cell line. We find IDH MT glioma cell lines are more sensitive

to unsaturated fatty acid treatment. Although HK252 cell line showed sensitivity to both saturated and unsaturated fatty acids. The fact that both TVB-2640 and VPA significantly decreases palmitic and stearic acid in HK157 suggests FASN may also have a role in regulating growth of IDH WT cell lines.

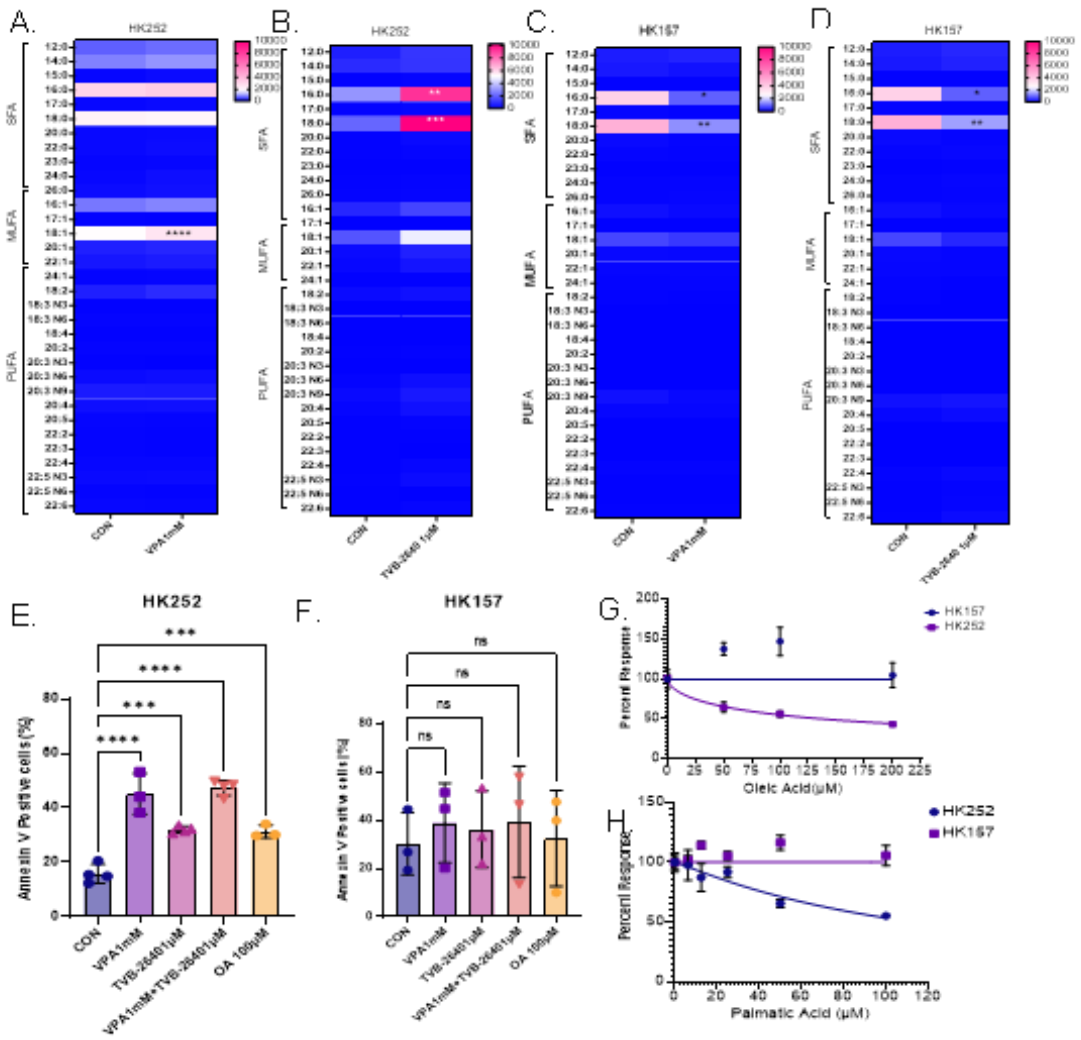

Fig6: VPA and TVB-2640 increases free fatty acid and promotes apoptosis in IDH MT GBM

A-D. Heatmap showing change in saturated and unsaturated free fatty acids after 4 days of treatment with VPA and TVB-2640

E-F. Flow cytometry quantification of Annexin V positive cells in HK252 and HK157

G. Dose response curve showing sensitivity of HK157, HK252 & BT142 to oleic acid

H. Dose response curve showing sensitivity of HK157, HK252 & BT142 to palmitic acid; 1-way ANOVA ****P value<0.0001; ***P value<0.001; Error bars ±SD

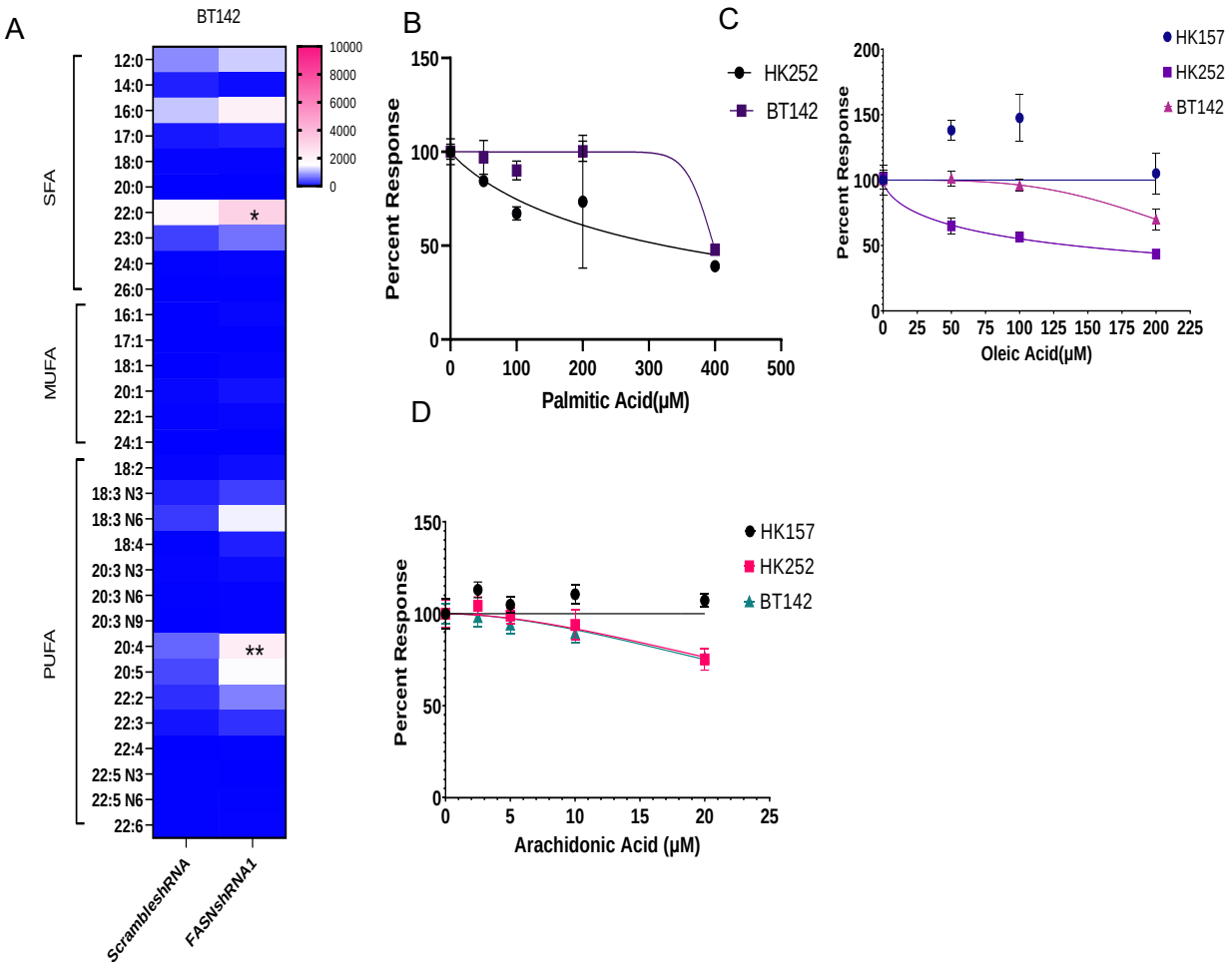

Supplementary Fig9: FASN knockdown increased free fatty acid in BT142

A. Heatmap showing change in free fatty acids after FASN knockdown in BT142

B. Dose response curve showing sensitivity of IDH MT and IDH WT cell lines to arachidonic acid

C. Dose response curve showing sensitivity of IDH MT and IDH WT cell lines to oleic acid

D. Dose response curve showing sensitivity of HK252 and BT142 cell lines to palmitic

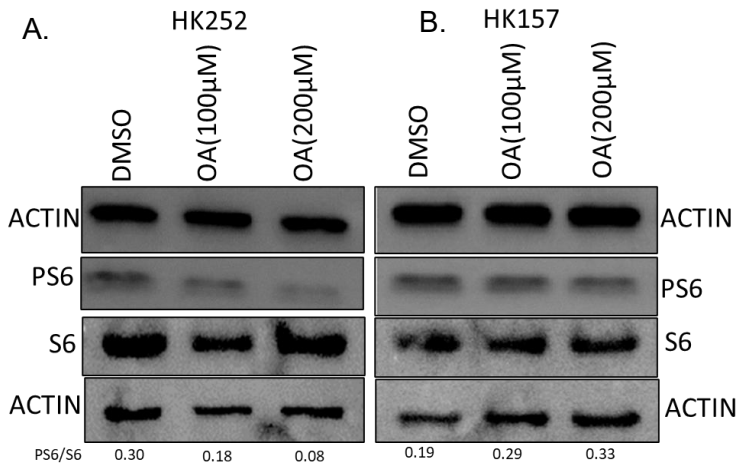

Supplementary Fig10: Oleic Acid (OA) decreases PS6 in HK252 but not HK157

A-B Representative Western Blot of HK252 and HK157 showing effect of OA treatment on PS6

Lipid droplets

We next tested the effect of VPA and TVB-2640 on lipid droplet formation in HK157, HK252 and BT142. We treated HK252, BT142, and HK157 with VPA, TVB-2640 and the combination for 4 days and stained them with Lipidspot™ a dye that specifically stains lipid droplets. In HK252 VPA treatment increased the number of lipid droplets per cell (Supplementary Fig11B, quantification,11H) compared to control (Supplementary Fig11A, 11H). TVB-2640 treatment inhibited VPA induced lipid droplet formation (Supplementary Fig11D, 11H). TVB-2640 decreased lipid droplets/ cell but compared to control did not reach statistical significance (Supplementary Fig11C). Oleic acid is a well-known lipid droplet inducer[84], to further validate our findings, we supplemented media with oleic acid and checked the effect of VPA and TVB-2640 on lipid droplet formation.

Oleic acid significantly increased lipid droplets in HK252 compared to control (Supplementary Fig11E, 11K). In HK252, combination of oleic acid with TVB-2640 decreased lipid droplets (Supplementary Fig11F, 11K) but combination of VPA and oleic acid increased lipid droplets (Supplementary Fig11G,11K). The combination of VPA and oleic acid induced a much more prominent and larger size lipid droplet formation (Supplementary Fig11G). In BT142 (Supplementary Fig11I) VPA and oleic acid (Supplementary Fig11L) also increased lipid droplets but did not reach statistical significance (low n) and TVB-2640 in combination with VPA (Supplementary Fig11I) and oleic acid (Fig11L) inhibited lipid droplet formation. Combination of VPA and oleic acid significantly increased lipid droplet formation in BT142 (Supplementary Fig11L). In HK157 oleic acid (Supplementary Fig10M) but not VPA (Supplementary Fig10J) significantly increased lipid droplets. Combination of VPA and oleic acid significantly increased lipid droplets and TVB-2640 inhibited lipid droplet formation (Supplementary Fig11M). Cholesterol esters and triacylglycerols are generally the main component of lipid droplets. We also measured cholesterol esters in the two cell lines HK252 and HK157. In HK252 VPA did not have a significant

effect on cholesterol esters, perhaps suggesting that the main content of lipid droplets is triacyl glycerides. However, TVB-2640 significantly decreased cholesteryl oleate (CE18:1) (Supplementary Fig12A.) In HK157 VPA but not TVB-2640 significantly decreased cholesteryl oleate (Supplementary Fig12B).

Thus far our data suggests both VPA and TVB-2640 alter free fatty acid composition, induces apoptosis, but diverges in the regulation of lipid droplets in IDH MT glioma cell lines.

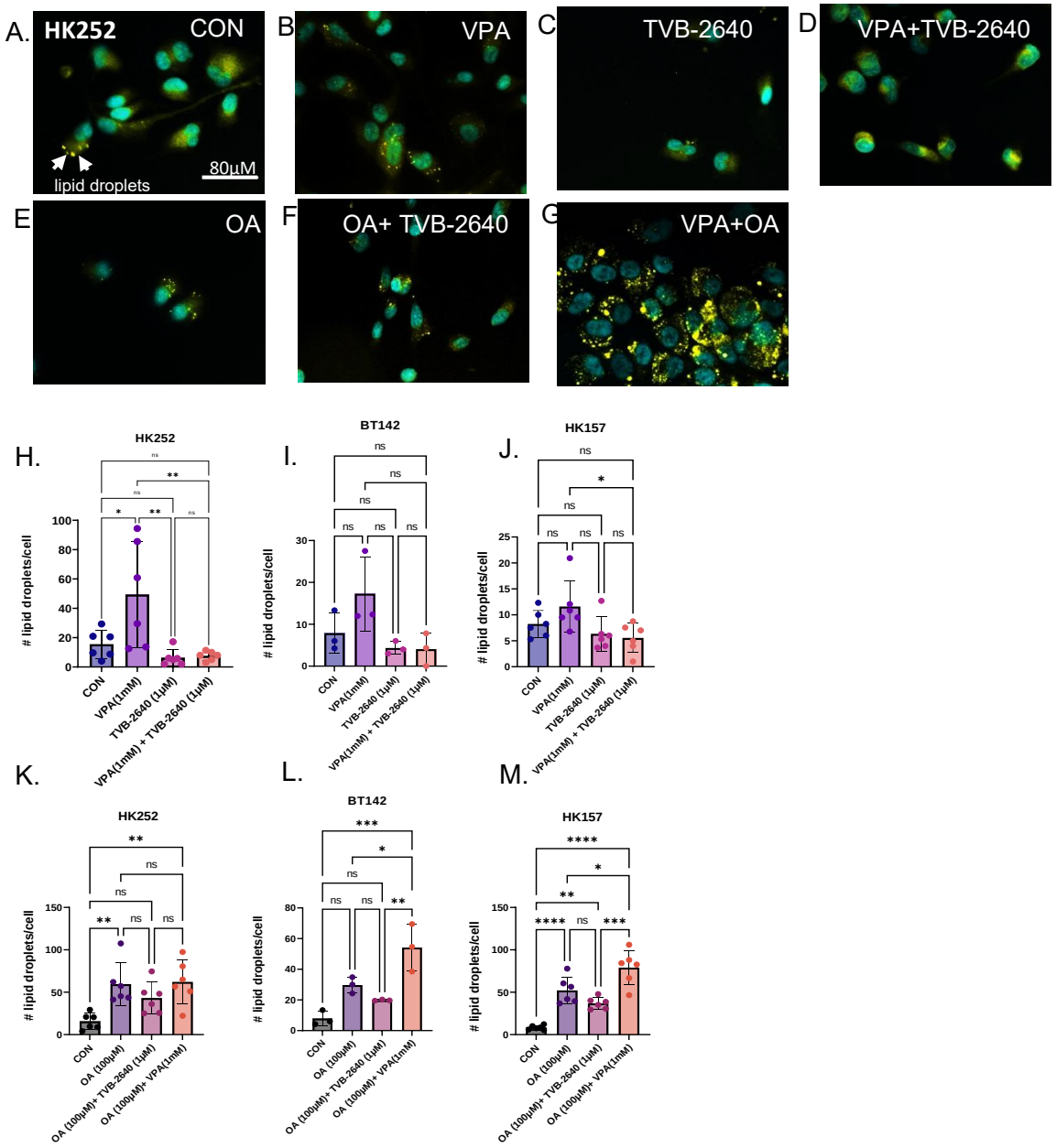

Supplementary Fig11: VPA increases lipid droplet formation whereas TVB-2640 inhibits lipid droplet formation.

A-G. Representative immunofluorescence images of lipid droplets in HK252 stained with Lipidspot™ .

H-M. Quantification of lipid droplets per cell in each condition. 1-way ANOVA ****P value<0.0001; ***P value<0.001; **P value<0.01; **P value<0.05; Error bars ±SD

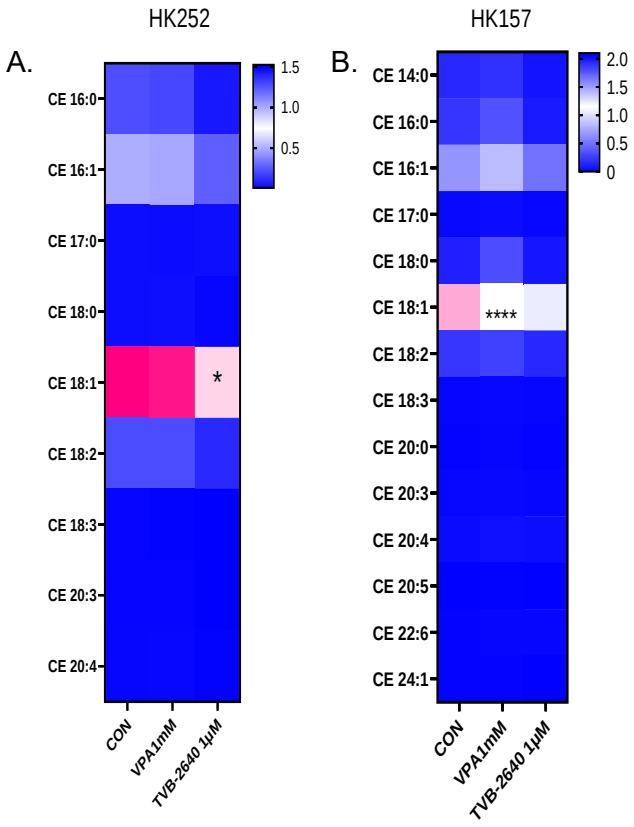

Supplementary Fig12: VPA and TVB-2640 alters CE 18:1 in HK252 and HK157

A-B. Heatmap showing change in cholesterol esters after 4 days of treatment with VPA and TVB-2640 in HK252 and HK157, respectively. 1-way ANOVA ****P value<0.0001; *P value<0.05

HDAC6 is involved in regulation of FASN in IDH MT glioma

Given that VPA is a known HDACi we next wondered whether any HDAC was involved in regulation of FASN. HDAC3 has been identified by previous studies to regulate deacetylation of FASN[85]. To address this, we took advantage of a recently published work that showed that HDAC1 and HDAC6 were important for growth regulation of IDH MT glioma[21]. We reanalyzed their RNA seq data on HK252 with different HDAC knockdowns and saw HDAC1 and HDAC6 knockdown had distinct effect on the transcriptome in HK252 cell line compared to other HDAC knockdowns (Fig7A). We next looked through the data to see if HDAC knockdown had any effect on FASN mRNA expression. The only HDAC knockdown that downregulated FASN mRNA expression was HDAC6 (Fig7B). Interestingly, SCD, the enzyme responsible for generating oleic acid was upregulated by several HDAC knockdowns. This suggests HDAC6 is involved in inducing some of the metabolic effects induced by VPA. Lastly, we independently knocked down HDAC6 in HK252 and saw a decrease in FASN protein expression (Fig7C). However, HDAC6 knockdown also downregulated HDAC9 and we cannot completely rule out the possibility that HDAC9 may also be important for FASN regulation or that HDAC6 and HDAC9 work together to regulate FASN expression in IDH MT glioma.

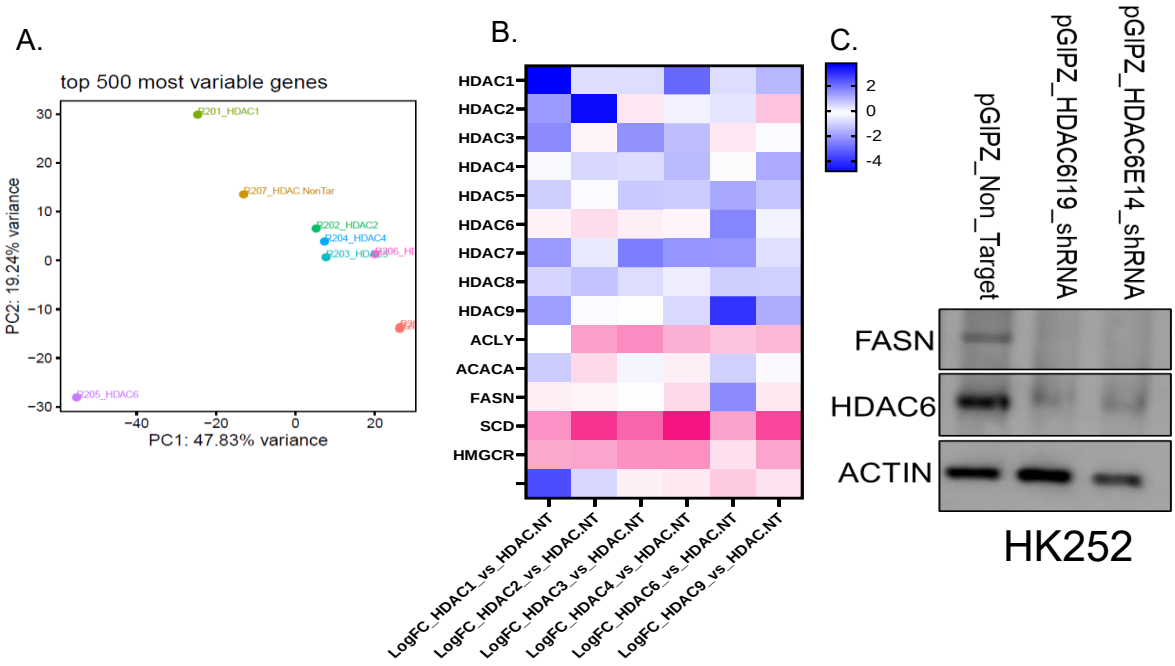

Fig7: Hdac6 knockdown downregulates FASN mRNA and protein expression in IDH MT cell line HK252

A. Principal Component Analysis (PCA) plot for HK252 with different HDAC knockdowns

B. Heatmap showing expression of HDAC and Lipogenic genes; FDR0.1

C. Representative WB showing FASN expression after HDAC6 knockdown in HK252

VPA prevents palmitate rescue and significantly improve survival of mice in combination with FASN knockdown

Thus far our data suggested although VPA downregulates FASN mRNA and protein expression some of the effects of VPA were distinct from FASN inhibitor TVB-2640. Therefore, we wanted to know what happens if we combine VPA with FASN inhibitor. We knocked down FASN in BT142 and saw that compared to non-target control FASN knockdown inhibited growth of BT142. Palmitate supplementation rescued some of the growth inhibitory effect of FASN knockdown. However, palmitate did not rescue the growth inhibitory effect of VPA. Interestingly,

in the presence of VPA exogenous palmitate could not rescue growth inhibitory effect of FASN knockdown in BT142 (Fig8A). We obtained similar results with TVB-2640. In the presence of VPA, palmitate could not rescue growth inhibitory effect of TVB-2640 in either HK252 (Fig8D) or BT142 (Fig8C). Glioma cells can source palmitate either through de novo lipogenesis or from the microenvironment[86]. Since VPA targeted FASN and prevented palmitate rescue we wondered how the combination of the two would affect tumor growth in vivo compared to FASN knockdown or VPA alone. In vivo in BT142, FASN knockdown significantly improved survival of mice but VPA was better than FASN knockdown in improving survival of mice in vivo (Fig8B). The combination of FASN knockdown and VPA was significantly better than VPA or FASN knockdown alone in improving survival of mice.

Finally, we tried to overcome the limitation of using hemizygous BT142 by overexpressing doxycycline (DOX) inducible WT IDH in BT142. Overexpression of WT IDH in hemizygous BT142 increased 2HG production (Supplementary Fig13A). To test the effect of TVB-2640 in the presence of high versus low 2HG we treated BT142 WT(OE) cell line with TVB-2640 in the presence of DOX and no DOX. The difference in TVB-2640 dose response curves with and without dox was barely significant(pval=0.0492) (Supplementary Fig13B). We knocked down FASN in BTWT(OE) model and saw a decrease in FASN protein expression with shRNA1 and shRNA3(Supplementary Fig13B). FASN knockdown inhibited growth of BTWT(OE) and surprisingly addition of DOX rescued some of the growth inhibitory effect of FASN knockdown. However, the addition of AG881 which blocks 2HG did not revert the rescue (Supplementary Fig13C). Hence, we hypothesized that the rescue was mediated by doxycycline and not heterozygous IDH mutation. We treated HK252 for a week with TVB-2640 with and without AG881 and saw no difference in the dose response curves (Supplementary Fig13D). Treatment of HK252 with DOX rescued some of the growth inhibitory effect of TVB-2640 in HK252 (Supplementary Fig13F). Luckily, we think we know why DOX rescued inhibitory effect of FASN. We assessed

lipid droplet content by flow cytometry in BT142WT(OE) model. Treatment of both BT142WT(OE) and hemizygous BT142 with DOX increased lipid droplet content (Supplementary Fig13G) and treatment with TVB-2640 lowered lipid droplet content. TVB-2640 inhibiting lipid droplets is similar to what we observed in our immunofluorescence quantification of lipid droplets in HK252, BT142, and HK157(Supplementary Fig11). We believe flow cytometry can be used reliability to assess lipid droplet content in cells. Based on this data we believe doxycycline induces lipid droplet formation and prevents free fatty acid induced lipotoxicity that happens as a result of FASN inhibition.

There is one discrepancy in our data that we still need to address. DOX rescued the effect of FASN knockdown in BT142WT(OE) model but only rescued the effect of TVB-2640 in HK252 but not in BT142WT(OE) with and without DOX. The question is why? Lipidomic on the BT142WT(OE) model answers the question (Supplementary Fig13I). We did lipidomic in the BT142WT(OE) model with VPA and TVB-2640 and the combination in the presence of DOX and no DOX. Treatment with both VPA and TVB-2640 instead of increasing, decreased free fatty acids in the BT142WT(OE) model. In HK252 TVB-2640 increased free fatty acids (Fig6B) and FASN knockdown in hemizygous BT142 (which is analogous to the BT142WT(OE) no DOX condition) also increased free fatty acids (Supplementary Fig9). Hence, the rescue with DOX is only seen when there is an increase and not a decrease in free fatty acids with FASN inhibition. Lastly, in the BT142WT(OE) model in the no DOX condition combination of VPA and TVB-2640 significantly increased the ratio of saturated to monounsaturated free fatty acids compared to control in the BT142WT(OE) no DOX condition suggesting combination of the two drugs VPA and TVB-2640 may be better at inducing or enhancing lipotoxicity in IDH MT gloma cell lines. Perhaps this is why why combination of FASN knockdown and VPA had the best effect on survival of mice in vivo.

However, due to the metabolic effect of DOX we conclude that using a dox inducible system to assess the effect of either VPA or TVB-2640 in vivo in the BT142WT(OE) model may not appropriately recapitulate the true effect of VPA and TVB-2640/FASNKD in heterozygous IDH MT glioma cells.

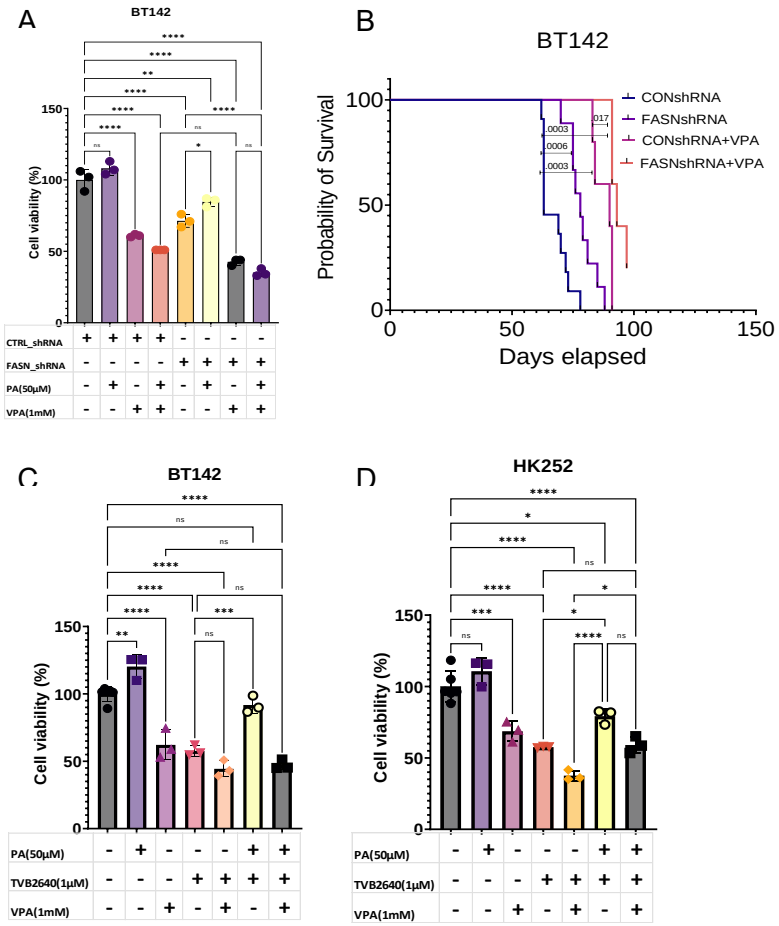

Fig8: VPA prevents palmitate rescue and significantly improves survival of mice in vivo alone and in combination with FASN knockdown

A. Relative growth of BT142 with ctrl non target shRNA and FASN shRNA treated with VPA and PA.

B. Kaplan-Meier survival curve for mice treated with either saline or VPA (300mg/kg) implanted with non-target BT142 or FASNshRNA1 KD BT142

C-D. Relative growth of BT142 and HK252 treated with VPA, TVB-2640, PA and combinations. 1-way ANOVA ****P value<0.0001; ***P value<0.001; **P value<0.01; *P value<0.05; Error bars ±SD

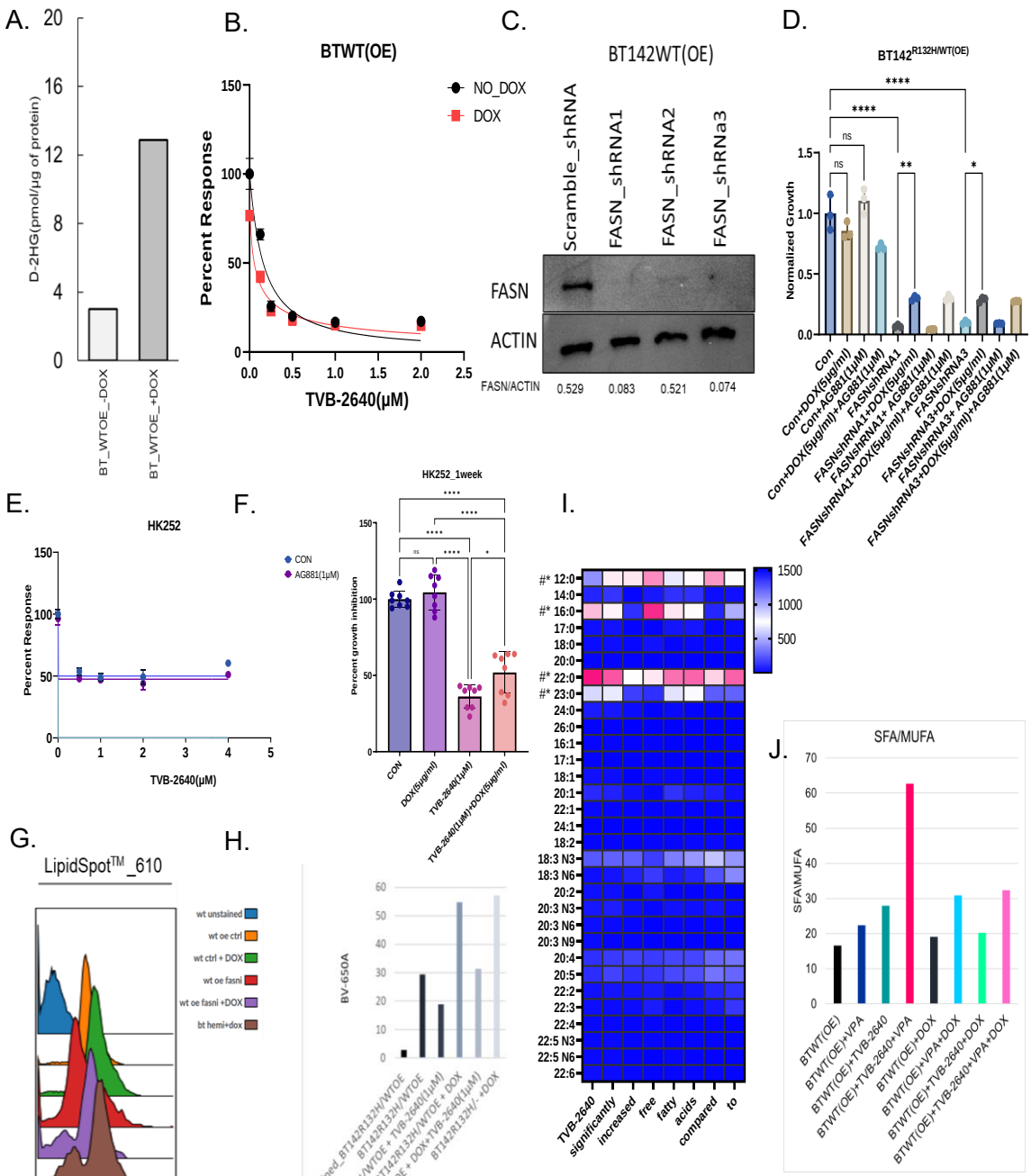
A.
D-2HG(pmol/µg of protein)
BT_WTOE_-DOX
BT_WTOE_+DOX
B.
BTWT(OE)
NO_DOX
DOX
Percent Response
TVB-2640(µM)
C.
BT142WT(OE)
Scramble_shRNA
FASN_shRNA1
FASN_shRNA2
FASN_shRNa3
FASN
ACTIN
FASN/ACTIN
0.529
0.083
0.521
0.074
D.
BT142R132H/WT(OE)
Normalized Growth
Con
Con+DOX(5µg/ml)
Con+AG6881(1µM)
Con+DOX(5µg/ml)+AG6881(1µM)
FASNshRNA1
FASNshRNA1+DOX(5µg/ml)
FASNshRNA1+ AG6881(1µM)
FASNshRNA1+DOX(5µg/ml)+AG6881(1µM)
FASNshRNA3
FASNshRNA3+DOX(5µg/ml)
FASNshRNA3+ AG6881(1µM)
FASNshRNA3+DOX(5µg/ml)+AG6881(1µM)
E.
HK252
Percent Response
TVB-2640(µM)
F.
HK252_1week
CON
AG881(1µM)
Percent growth inhibition
CON
DOX(5µg/ml)
TVB-2640(1µM)
TVB-2640(1µM)+DOX(5µg/ml)
I.
TVB-2640 significantly increased free fatty acids compared to
J.
SFA/MUFA
BTWT(OE)
BTWT(OE)+VPA
BTWT(OE)+TVB-2640
BTWT(OE)+TVB-2640+VPA
BTWT(OE)+DOX
BTWT(OE)+VPA+DOX
BTWT(OE)+TVB-2640+DOX
BTWT(OE)+TVB-2640+VPA+DOX
G.
LipidSpot™_610
wt unstained
wt oe ctrl
wt ctrl + DOX
wt oe fasni
wt oe fasni +DOX
bt hemi+dox
BV650-A
H.
BV-650A
Unstained_BT142R132H/WTOE
BT142R132H/WTOE
BT142R132H/WTOE + TVB-2640(1µM)
BT142R132H/WTOE + DOX
BT142R132H/WTOE + DOX+TVB-2640(1µM)
BT142R132H/- +DOX

Supplementary fig13: Doxycycline rescues growth inhibitory effect of FASN inhibition by inducing lipid droplet formation

A. D-2HG content inducing WT expression with DOX(5µg/ml) for three days. B. TVB-2640 dose response in BT142WT(OE) with and without DOX induction C. Representative WB FASN knockdown in BT142WT(OE). D. Growth response in BT142 WT(OE) after FASN knockdown with DOX and AG881. E. HK252 dose response curve for TVB-2640 with and without AG881(1µM). F. Combination of DOX with TVB-2640 in Hk252 G. Lipid droplet staining in BT142WT(OE) with LipidSpot™ measured by flow cytometry. H Median peak intensity of from graph in I. Heatmap of free fatty acid panel with VPA, TVB-2640, and combination in BTWT(OE) with and without DOX. J Ratio of SFA/MUFA calculated using the data in I. 1-way ANOVA ****P value<0.0001; ***P value<0.001; **P value<0.01; **P value<0.05; Error bars ±SD. #* indicates significant difference in fatty acids between conditions (detailed explained in text)

Discussion

In this study we show that both VPA and FASN inhibitor TVB-2640 inhibited growth of IDH MT glioma cell lines in vitro and FASN knockdown and VPA improved survival of mice in vivo. Mechanistically, treatment with VPA condenses the chromatin and decreases promoter chromatin accessibility of multiple lipogenic genes. We focused on one of those lipogenic candidates FASN and show that VPA targets FASN via inhibition of the mTOR pathway. Both VPA and TVB-2640 altered the lipidome by altering free fatty acids and lipid droplet formation and induced apoptosis in IDH MT glioma cells. We further identified HDAC6 to be involved in regulation of FASN mRNA and protein expression in IDH MT GLIOMA. Lastly, we propose that combination of VPA and FASN inhibitor may be better at targeting IDH MT glioma due to enhanced lipotoxicity.

Effect of VPA on IDH MT GBM cellular growth

We tested multiple HDACis in primary IDH MT glioma cell lines and found that IDH MT GBM cell lines were most responsive to VPA. Several studies in recent years have reported similar findings with different HDACis. Overexpression of R132H in NHA, LN229, U87 & M70 astrocyte cell lines in two separate studies sensitized cell lines to HDACis invitro[55,87]. Three studies using primary IDH MT GBM cell lines showed sensitivity of IDH MTglioma cell lines towards panobinostat, vpa, and belinostat, invitro[21,24,25]. Although in our hands MT cell lines did respond to panobinostat and belinostat we found primary IDH MT cell lines to be most sensitive to VPA treatment. None of the studies above showed efficacy of any of these HDACis as a monotherapy in vivo against IDH MT glioma so we cannot directly compare our in vivo findings with their studies. A report from a phase I clinical trial however found in a single patient, IDH MT glioma in combination with standard care of treatment was more sensitive to belinostat treatment than IDH WT GBM[87].

Effect of VPA on gene expression and chromatin

VPA is a multifaceted drug that directly target HDACs[75] and in line with its role as a HDACi increased H3K27ac in a IDH MT and a IDH WT cell line. We did notice that VPA increased histone acetylation in HK252 much more than IDH WT cell line HK157. Sears et al. reported similar results and showed that HDACis preferentially increased H3 acetylation in IDH MT glioma cell lines. Increased histone acetylation is generally associated with increased transcription and unsurprisingly VPA treatment both short and long term upregulated many genes and downregulated a small number of genes. The fact that VPA treatment resulted in chromatin condensation is unexpected. One possibility is that VPA has indirect effect on histone and DNA methylation. Short and long term VPA treatment has been found to modify DNA methylation in glioma stem cells[88]. Lunke et al. recently showed that VPA promoted both histone acetylation and deacetylation, and the increase in histone acetylation with VPA is regional[89]. Hence, multiple levels of chromatin modification by VPA may ultimately be responsible for chromatin condensation seen with VPA. One interesting observation that we made is that GFAP expression went up after long term treatment in one IDH MT cell line but not another. This suggests long term VPA treatment may have the potential to promote differentiation in some IDH MT glioma but not all IDH MT tumors. Similar results were reported by a group that treated WT glioma cells with VPA for a long term[88]. GFAP expression can be promoted in IDH MT GLIOMA cells using 5-azacytidine[14]. In an IDH1 mutant glioma xenograft model it took 7 weeks of continuous treatment with 5-azacytidine to promote cellular differentiation in vivo. We did not see induction of GFAP in one of our cell lines with three weeks of treatment. It is possible that some cell lines require longer treatment than others. Combining VPA with 5-azacytidine to promote differentiation of IDH MT cells could be a viable future strategy.

Effect of VPA on Lipidome and Lipogenic enzymes

Structurally VPA itself is a short chain fatty acid and perhaps it is not that surprising that VPA altered lipid metabolism. The most information that we have regarding VPA, and lipid metabolism comes from studies looking at VPA induced hepatoxicity. Xu et al. using untargeted lipidomics compared serum from epileptic patients with normal liver function with epileptic patients with abnormal liver function (ALF)[90]. In ALF patients VPA decreased ceramides, sphingomyelin, and lysophosphatidylcholines and significantly increased triglycerides. In LN2 cell line VPA treatment significantly increased triglycerides and shifted the ratio of free fatty acids towards unsaturated fatty acids although in their study the shift did not reach statistical significance. In parallel to their finding, in IDH MT gloma cell line we saw VPA treatment significantly increased the ratio of monounsaturated to saturated fatty acid. Interestingly, one study analyzed free fatty acids and lipid profile in epilepsy patients receiving VPA and they found a positive correlation between concentration of VPA and oleic acid in patients with uncontrolled epilepsy[91] suggesting increase in oleic acid with VPA treatment may not simply be an in vitro effect.

Another study with HepaRG cell line saw an increase in triglyceride metabolism and increase in lipid droplet content[92] with VPA treatment. Similarly, in our study we saw an increase in lipid droplets in IDH1 MT glioma cell lines with VPA treatment. Interestingly, with VPA treatment Grunig et al. saw a decrease in mRNA expression for FASN and an increase in mRNA expression for DGAT2, an enzyme involved in triglyceride synthesis. Surprisingly, we also saw a significant increase in DGAT2 mRNA expression with VPA treatment in the IDH MT glioma cell lines and a significant decrease in FASN mRNA expression. One potential hypothesis is that VPA increases triglyceride synthesis as evident by increased lipid droplet formation via DGAT2 in our IDH MT cell lines and in order to accommodate for increased triglyceride synthesis IDH MT glioma inhibits the de novo lipogenesis pathway hence we see a massive downregulation of lipogenic genes in IDH MT glioma.

Although we cannot completely rule out that HDACs don't play a role in this process. Acetylome studies have found that almost all metabolic enzymes involved in glycolysis, TCA cycle, urea, and fatty acid metabolism are acetylated[93,94]. HDACis can induce lysine acetylation in non-histone proteins which can then alter cell signaling, differentiation and apoptosis in cells[95]. Acetylation have been found to result in proteasomal degradation of lipogenic enzyme such as FASN[85]. Deletion of HDAC3 in the liver has been found to reroute precursors towards lipid synthesis and the increased production of lipids further resulted in sequestration into lipid droplets[96]. This suggests HDAC inhibition is potentially the first step in this signaling cascade. VPA inhibits HDACs, inhibition of HDACs reroutes metabolites toward triglyceride synthesis which ultimately results in increased formation of lipid droplets and inhibition of the de novo lipogenesis pathway.

Our ATAC seq data showed loss of chromatin accessibility at promoters of lipogenic genes. In prostate cancer cells transcription factor HOXB13 recruits HDAC3 to the promoter of FASN and downregulates FASN and ultimately de novo lipogenesis[72]. Although we did not see motif enrichment for HOXB13 we did see an increase in HOXB13 mRNA expression with VPA treatment. Some of our preliminary data suggested overexpression of HOXB13 killed IDH MT cells however we need to further validate the finding. In our ATAC seq data we did identify NF-YA and NFYB as potential lipogenic transcription factors. Activation of NF-YA inhibits fatty acid biosynthesis and has been shown to directly bind to the promoters of lipogenic genes such as FASN and SCD[77]. NF-Y can also associate with HDAC1 and regulate gene transcription[97]. It is possible HDAC and NF-Y interact with each other at the promoter of lipogenic genes modulate chromatin accessibility by either deacetylation or methylation and ultimately inhibits transcription of lipogenic genes.

Effect of VPA on the mTOR pathway

The status of mTOR pathway in IDH MT GLIOMA is controversial. In 2015, Fu et al. found 2-HG inhibits ATP synthase and mTOR signaling in IDH MT gliomas[98]. In 2016, Carbonneau et al. found 2HG activates mTOR signaling in IDH MT gliomas and acute myeloid leukaemias by inhibiting lysine demethylase KDM4A[99]. Inhibition of KDM4A decreases DEPTOR stability and activates mTOR. In 2019, a study showed inhibition of mTOR signaling lowered 2HG in orthotopic IDH MT xenograft model and improved survival of mice[100] . In 2022, Mohamed et al. analyzed a cohort of 132 IDH-mutant diffuse glioma and found at least 43.9% of tumors had active mTOR signaling and mTOR signaling activity increased with tumor grade [101]. The fact that mTOR signaling is up in some IDH MT tumors suggests mTOR pathway may be a potential target for some if not all IDH MT tumors.

VPA promotes differentiation of neural stem cells into neurons through activation of the mTOR pathway[102] and VPA inhibits phosphorylation of mTOR, AKT, S6 and promotes autophagy in glioma[103], gastric[104] and prostate cancer cell lines[105]. In our study we found VPA inhibited the mTOR signaling pathway and we think this is at least partly due to alteration in lipid metabolism. mTOR is a multifaceted protein and can sense amino acids[106] and lipids[107]. In Kras-driven cancer cell lines oleic acid induced mTORC1 and mTORC2 activity that was abrogated by knockdown of mTOR partners rictor and raptor[107]. VPA treatment significantly increased free oleic acid in IDH MT glioma cell line HK252. We also saw a decrease in mTOR activity in HK252 but not HK157 with exogenous oleic acid treatment. DEPTOR is a negative regulator of mTOR and DEPTOR-mTOR signaling is important for lipid metabolism[108].With VPA treatment we saw an increase in mRNA expression for DEPTOR in IDH MT glioma cell lines suggesting DEPTOR-mTOR interaction might be involved in regulating the mTOR pathway. Unfortunately, DEPTOR expression was low in IDH MT glioma cell lines and was hard to detect by WB so we could not validate whether DEPTOR protein goes up with VPA treatment.

Lastly, we did notice that HDAC1 knockdown in HK252 decreased Ras homolog enriched in brain (RHEB) expression. RHEB is an mTOR activator and inhibition of HDAC1 may downregulate RHEB and inhibit mTOR signaling. However, we did not see a significant change in RHEB mRNA expression with VPA treatment. Taken together increase in oleic acid and potential interaction between DEPTOR-mTOR may be involved in regulating mTOR pathway in IDH MT glioma with VPA treatment.

Effect of TVB-2640 and palmitate on growth of IDH MT GLIOMA

In our study we tested the effect of TVB-2640 in 2 IDH WT and 2 IDH MT GLIOMA cell lines. We find a wide range of responses to TVB-2640 even in the small panel of cell lines tested. There is metabolic heterogeneity in cancer cells and glycolytic versus lipogenic cell lines can respond differently to metabolic inhibitors[109]. Both IDH MT cell lines HK252 and BT142 had a lower IC50 for TVB-2640 compared to WT HK157. Several studies have suggested IDH MT cells limit de novo lipogenesis and instead use NADPH for 2HG[73,74]. It is possible that because de novo lipogenesis is already limited in MT cell lines MT cell lines have increased sensitivity to FASN inhibition. But the lack of dose dependent response in HK252 suggests that MT cell lines perhaps can and tries to compensate for FASN inhibition. In vivo cancer cells uptake palmitate from the microenvironment. Interestingly, HK252 showed sensitivity to both FASN inhibition and palmitate. Perhaps cancer cell lines that are sensitive to both palmitate and FASN are better candidates for FASN inhibitors. Finally, we saw a decrease in cell cycle genes with TVB-2640 which was rescued by palmitate supplementation. This suggests the effect of FASN on cell cycle genes is due to palmitate deprivation. In summary, blocking FASN and palmitate uptake from the environment is a better way of attacking glioma cell lipid metabolism.

Effect of TVB-2640 on free fatty acids and lipid droplet formation

In HK252, TVB-2640 significantly increased free fatty acids whereas in HK157 TVB-2640 significantly decreased free fatty acids. Is the increase in free fatty acid a compensatory or kill me mechanism? Our data suggests it is the latter. We unexpectedly discovered doxycycline rescued some of the growth inhibitory effect of TVB-2640 in HK252. Cancer cells generally form lipid droplets to prevent ER stress and lipotoxicity[80.] We think doxycycline decreases excess free fatty acids by promoting lipid droplet formation and thereby rescues some of the inhibitory effect of TVB-2640. The effect of doxycycline on cell metabolism has been reported by others. In a panel of human cell lines doxycycline increased glycolytic metabolism[110]. However, the effect of doxycycline on lipid droplets has never been reported.

Nonetheless, we don't see a complete rescue and it is possible that increase in free fatty acids is indeed a compensatory mechanism. In breast cancer cells FASN inhibition have been found to increase unsaturated fatty acids, ceramides, and diacylglycerols[111]. In prostate cancer cells inhibition of FASN by multiple FASN inhibitors increased synthesis of long chain unsaturated fatty acids and phospholipids[112]. This suggests cancer cells potentially upregulate multiple other metabolic pathways to compensate for FASN inhibition and this may be conserved among multiple cancer types.

Lastly, we saw a decrease in lipid droplet formation and a decrease in cholesterol oleate CE 18:1 with FASN inhibition in IDH MT cell line HK252 but not WT cell line HK157. Cancer cells can break down preexisting lipid droplets to release free fatty acids to meet their metabolic demand[113] which might explain the decrease in cholesterol oleate. Acyl Coa: diacylglycerol acyltransferase (DGAT) enzymes, DGAT1 and DGAT2 are important for triacylglycerol synthesis and lipid droplet formation[114]. RNA seq data with TVB-2640 showed TVB-2640 downregulated mRNA expression

of DGAT2 in both BT142 and HK252. This suggests the inhibition of lipid droplets may be mediated by DGAT2.

Role of HDAC6 in FASN regulation

To the best of our knowledge no study till date has made any association between HDAC6 and FASN. Two studies, however, associated HDAC3 with FASN. The first study showed HDAC3 is responsible for deacetylation of FASN[85]. The second study reported that in androgen independent prostate cancer cells homeobox gene HOXB13 recruits HDAC3 at lipogenic enhancers to suppress FASN and inhibit de novo lipogenesis[115]. However, in HK252 knockdown of HDAC3 did not have any effect on FASN mRNA expression but HDAC3 mRNA expression went up with HDAC6 KD. Interestingly, mRNA expression of SCD the enzymes responsible for oleic acid synthesis went up with several HDAC knockdown suggesting HDACs are involved in regulation of multiple lipogenic enzymes and the effect of VPA on the chromatin and the lipidome are not necessarily two separate entities but rather connected with each other.

Rationale for combination of VPA and TVB-2640

In this study we showed that combination of FASN inhibition with VPA is better at improving survival of mice in vivo compared to either alone. There are several potential explanations for this observation. We identified several positive and several negative aspects of both VPA and TVB-2640. Our analysis suggested combining VPA with TVB-2640 together may overcome some of the limitations of the two drugs. VPA increased lipid droplet formation potentially via upregulation of DGAT2 which might be a mechanism to prevent lipotoxicity and prevent cancer cell death. Whereas TVB-2640 inhibited lipid droplet formation potentially by inhibition of DGAT2. The combination of the two drugs decreased lipid droplet formation as seen in Supplementary Fig 11. In the BT142WT(OE) no DOX condition combination of VPA with TVB-2640 showed greater alteration in the ratio of saturated to monounsaturated free fatty acids; almost 3 times higher than

control (Supplementary Fig13I) suggesting that the two drugs may work together to drive lipotoxicity in IDH MT GLIOMA. Addition of dox with VPA and TVB-2640 in the BT142WT(OE) model decreased the ratio of saturated to monounsaturated free fatty acids further suggesting doxycycline prevents lipotoxicity.

Altogether, our study reveals both metabolic vulnerability and flexibility of IDH MT glioma cells. We learn that there is complex interaction between the chromatin and the lipidome and they can regulate each other. Due to the metabolic flexibility of IDH MT glioma we propose combination of multiple drugs might be a better way of targeting IDH MT glioma.

Methods

All experiments in this study comply with relevant ethical regulations and have been approved by the UCLA Institutional Review Board. Protocols for animal studies were approved by the institutional animal care and use committee at UCLA. All patient samples were de-identified and collected under informed consent and with the approval of UCLA Medical Institutional Review Board.

Experimental cell lines and drugs

The primary patient derived IDH WT and IDH MT cell lines were established in our laboratory and cultured in serum free condition as previously described[61]. The murine glioma cell lines (NRAS G12V-shp53-shATRX-IDH1 wildtype; NPAC54B) and (NRAS G12V-R132H-shp53-shATRX-IDH1 mutant; NPAIC1) were obtained from Dr. Maria Castro and cultured in the same media as patient-derived gliomaspheres. The cultures were regularly checked for mycoplasma. The following drugs were used for the experiments. Valproic acid sodium salt,98% (Sigma-Aldrich, P4543-10G), panobinostat (Cayman, 13280), Belinostat (PXD101) (Sellechckem S1085), TVB-2640 (Sellechckem S9718), Oleic Acid (Cayman Chemical, 90260), Palmitic Acid (Sigma, 57-10-3), Arachidonic Acid (Cayman 506-32-1), Rapamycin (LC laboratories, R5000), Vorasidenib (AG-881)(Selleck Chemicals, S8611)

Animal Studies

Studies did not discriminate sex, and both male and females were used. Strains: 8 to 12-week-old NOD-SCID gamma null (NSG) mice (NOD.Cg-*Prkdc*^{scid} *Il2rg*^{tm1Wjl}/SzJ Jackson Laboratory, 00557) were used to generate tumors from a patient-derived glioma line BT142. C57BL6 (Jackson Laboratory, 000664) were used to transplant a murine NPAC54B and NPAIC1 as described previously[116]. Firefly-luciferase-GFP BT142 (1X105) tumor cells were injected intracranially into the neostriatum of mice. 1 week after tumor cell line implant mice were treated

with VPA (300mg/kg) of body weight twice a day every day of the week. For FASN knockdown and VPA experiment mice were treated with VPA (300mg/kg) of body weight twice a day 5 days a week. AG881 (2mg/kg) was dissolved in sucrose and given by oral gavage twice a day every day of the week. Treatment continued until the animal reached the endpoint. Tumor growth was monitored once a week by measuring luciferase activity using IVIS Lumina II bioluminescence imaging. Survival: Mice were euthanized if they looked hunched, lost significant body weight, or showed fur changes and decreased activity than normal for survival analysis.

Bulk RNA sequencing and analysis

Qiagen RNeasy microkit was used for RNA extraction from gliomasphere. RNA quality was assessed using Bioanalyzer and only samples with a RIN score >8.0 were sequenced. RNA samples were pooled and barcoded, and libraries were prepared using TruSeq Stranded RNA (100 ng) + Ribozero Gold. Paired-end 2X75bp reads were aligned to the human reference genome (GRCh38.p3) using the STAR spliced read aligner (v 2.3.0e). Total counts of read fragments aligned to known gene regions within the human hg38 refSeq reference annotation was used as the basis for the quantification of gene expression. Differentially expressed genes were identified using EdgeR Bioconductor R-package, which are then considered and ranked based on False Discovery Rate (FDR Bejamini Hochberg adjusted p-values of ≤ 0.01(not 0.1?)). Gene Set Enrichment Analysis (GSEA) was carried out to determine the gene signatures differentially regulated in control and radiated cells and represented as heatmaps. R-Package V.3.2.5 (The R project for Statistical Computing, https://www.r-project.org/) was used to generate the PCA plots and heatmaps.

ATAC sequencing and analysis

HK252 and HK211 were treated with VPA(1mM) and C35(10uM) for three weeks and cell pellet was submitted to TCGB core for processing according to the protocol, Corces et al. 2017[117].

ATAC-Libraries from each condition were sequenced on NextSeq 500 High Output Kit v2 (150 cycle, FC-404-2002, Illumina). Alignment of reads was carried out using the Burrows-Wheeler Aligner mem using hg19 assembly. Peak calling was performed using MACS2 (with parameter setting –nomodel –shift 75), and differential peak analysis using featureCount and DESeq2 (default setting). Motif analysis and peak annotation was done using HOMER and GO analysis using HOMER (http://homer.ucsd.edu/homer/) and EnrichR (https://maayanlab.cloud/Enrichr/). UCSC Genome Browser was used to determine whether open regions displayed H3K27Ac and conserved TF binding sites. Integrated Genome viewer (IGV) was used to represent the peaks/open regions.

Free fatty acid and cholesterol ester panel GC-MS & Analysis

1X10^6 million cells per sample per condition in triplicate were submitted to UCSD Lipidomic Core. Samples were prepared using previously published protocol Quehenberger et al. (2010) and analyzed at UCSD Lipidomics Core.

Cell viability assay

WT and MT cells were plated at a density of 5000 cells per well in 96-well plates. Proliferation was assessed 7 days after treatment with respective drugs using CellTiter-Glo® luminescent Cell Viability Assay (Fisher Scientific, PRG9242). The luminescence signal was measured in a luminometer, on day 0 and day7. Luminescence signal was normalized to initial reading at day0.

Western blot assay

At experimental end points cells were collected and lysed in RIPA buffer with protease and phosphatase inhibitors. Cells were kept on ice for 10 mins and centrifuged at full speed for 5 minutes. Protein concentration was measured by Bradford assay using a BSA standard. Protein lysates were run on a SDS-PAGE on 4%–12% gradient polyacrylamide gel (Thermo-fischer

Scientific) and transferred onto nitrocellulose membranes. Blots were incubated with primary antibody diluted in 5% milk overnight. Blots were washed and incubated with HRP-conjugated secondary antibodies. Quantitation of protein levels was performed in ImageJ by normalizing to loading control, β-actin.

Annexin V/7ADD assay

Cells were treated for 4 days with VPA and TVB-2640 and cells were prepared according to manufacturer's instruction for Biotium Annexin V and 7-AAD Apoptosis Kit and acquired by flow cytometry within an hour.

Lipid droplet staining and flow cytometry

LipidSpot Lipid Droplet Stain 647 was used to stain lipid droplets in gliomasphere cultures. Cells were plated on a 24 well dish in Cultrex UltiMatrix covered coverslips. Cells were treated with drugs for 4 days and at experimental endpoint, media was removed, cells were washed, and incubated with 1X dye diluted in DPBS for 15 min at 37º C. After 15 mins the dye was removed, and cells were fixed with 4% PFA. Nuclei were stained with Hoechst and mounted on coverslips with vector shield. Coverslips were imaged and analyzed using Image J.

For flow cytometry quantification at experimental endpoint media was removed and cells were incubated with 1X dye diluted in DPBS for 30 min at 37º C. After 30 min cells, the dye was removed, cells were dissociated into single cells and acquired using flow cytometry.

shRNA and CRISPR/Cas9 Lentiviral Knockdown

The following plasmids were used for knockdown experiments Scramble shRNA plasmid # 1864 (Addgene); FASN shRNA1 plasmid # 82327(Addgene); FASN shRNA2 _ TRCN0000002125 (Horizon); FASN shRNA2 _ TRCN0000002126 (Horizon); FASN_shRNA3_TRCN0000002127 (Horizon); HDAC6_shRNAI19(MSSR CORE); HDAC6_shRNA_E14(MSSR CORE);

sgPTEN1(gcatatttattaca^tcgggg) EXON5; sgPTEN3(ccacac^gggaagacaa) _EXON7. These plasmids were transfected into 293T cells along with a 2nd generation viral DR8.74 package and VSV-g envelope for production of lentivirus. Cells were infected with lentivirus and puro selected for a week before doing growth experiments. For cells infected with FASN shRNA media was supplemented with palmitic acid (50μM) along to puromycin to prevent all knockout cells from dying.

Statistical Analysis

All data are expressed as mean ± SD. *P* values less than 0.05 were taken as significant and were calculated in Graph Pad Prism 9.0 using one-way ANOVA for multiple comparison with Bonferroni correction, followed by post-hoc t-test. Log-rank analysis was used to determine the statistical significance of Kaplan-Meier survival curves. R-package was used for statistical analysis of sequencing experiments. Schematics used in the figures were generated in Biorender.

Chapter 3

Summary and Perspective

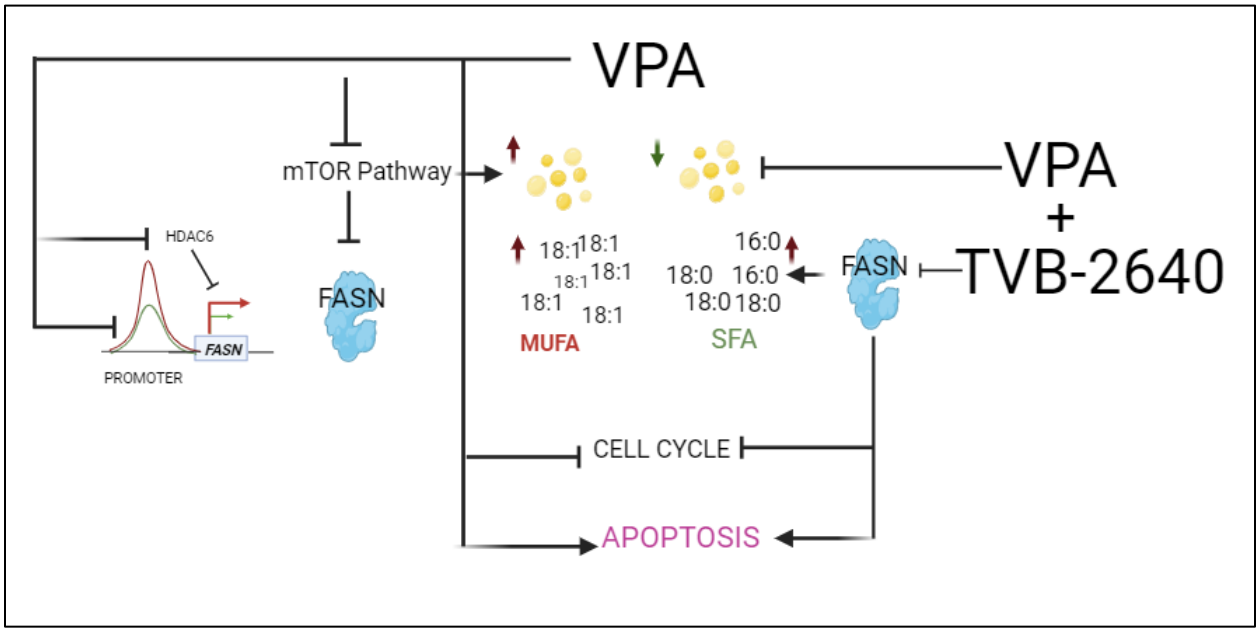

Figure 1: Proposed mechanism of action of VPA and TVB-2640 in IDH MT

Altogether, our study shows VPA reprograms both the chromatin and the lipidome of IDH1 MT glioma. Our in-depth analysis suggests VPA has many targets and may ultimately work through multiple mechanisms to inhibit growth of IDH1 MT gliomas. We find some of the mechanistic actions of VPA on both IDH1 WT and IDH1 MT are the same while others are different. VPA increased transcription and led to chromatin condensation in both IDH1WT and IDH1 MT cell lines. However, we find the downstream effect on the lipidome is what distinguished IDH1 MT from IDH1 WT. Both VPA and the FASN inhibitor TVB-2640 inhibited growth of both IDH1 WT cell line HK157 and IDH1 MT cell line HK252, but both drugs induced apoptosis only in the IDH1 MT cell line but not in the IDH1 WT cell line. We also find that only IDH1 MT and not IDH1 WT is sensitive to oleic acid treatment and while VPA increased free oleic acid in IDH1 MT it decreased saturated free fatty acid in IDH1 WT cell line. Lastly, we also find VPA may mediate some of its effect on lipogenic enzymes via HDAC6. Interestingly, HDAC6 knockdown inhibited

the growth of only IDH1 MT cell line HK252 but not IDH1 WT cell line HK157. We conclude VPA's unique effect on the IDH1 MT lipidome may ultimately make them more sensitive to VPA than IDH1 WT.

Lipogenic enzymes can be significant therapeutic targets in cancer, but it is important to note that cancer cells can use multiple metabolic pathways for survival. In our study for instance, we found that only selective inhibition of FASN by TVB-2640 upregulated cholesterol metabolism in IDH1 MT gliomas. VPA, on the other hand, targeted enzymes that are important for both lipogenesis and cholesterol metabolism. Perhaps VPA's pleotropic targets are more of an advantage than disadvantage for the treatment of IDH1 MT gliomas. Nonetheless, we found that VPA increased lipid droplet formation which might be a resistance mechanism and interestingly combination of TVB-2640 with VPA inhibited lipid droplet formation. In vivo, the combination of VPA with FASN knockdown was also better than VPA and FASN knockdown alone in improving survival of mice. Hence, we think in order to overcome the metabolic flexibility of cancer cells dual targeting of FASN by both VPA and TVB-2640 is potentially a better therapeutic approach for IDH1 MT glioma.

References

1. Noushmehr, H. *et al.* Identification of a CpG island methylator phenotype that defines a distinct subgroup of glioma. *Cancer Cell* **17**, 510–22 (2010).
2. de Souza, C. F. *et al.* A Distinct DNA Methylation Shift in a Subset of Glioma CpG Island Methylator Phenotypes during Tumor Recurrence. *Cell Rep* **23**, 637–651 (2018).
3. Flavahan, W. A. *et al.* Insulator dysfunction and oncogene activation in IDH mutant gliomas. *Nature* **529**, 110–114 (2016).
4. Chaligne, R. *et al.* Epigenetic encoding, heritability and plasticity of glioma transcriptional cell states. *Nature Genetics 2021 53:10* **53**, 1469–1479 (2021).
5. Xu, W. *et al.* Oncometabolite 2-Hydroxyglutarate Is a Competitive Inhibitor of α-Ketoglutarate-Dependent Dioxygenases. *Cancer Cell* **19**, 17 (2011).
6. Xu, W. *et al.* Oncometabolite 2-Hydroxyglutarate Is a Competitive Inhibitor of α-Ketoglutarate-Dependent Dioxygenases. *Cancer Cell* **19**, 17–30 (2011).
7. Figueroa, M. E. *et al.* Leukemic IDH1 and IDH2 Mutations Result in a Hypermethylation Phenotype, Disrupt TET2 Function, and Impair Hematopoietic Differentiation. *Cancer Cell* **18**, 553–567 (2010).
8. Modrek, A. S. *et al.* Low-Grade Astrocytoma Mutations in IDH1, P53, and ATRX Cooperate to Block Differentiation of Human Neural Stem Cells via Repression of SOX2. *Cell Rep* **21**, 1267–1280 (2017).
9. Lopez-Bertoni, H. *et al.* Sox2 induces glioblastoma cell stemness and tumor propagation by repressing TET2 and deregulating 5hmC and 5mC DNA modifications. *Signal Transduction and Targeted Therapy 2022 7:1* **7**, 1–12 (2022).
10. Tiburcio, P. D. B., Locke, M. C., Bhaskara, S., Chandrasekharan, M. B. & Huang, L. E. The neural stem-cell marker CD24 is specifically upregulated in IDH-mutant glioma. *Transl Oncol* **13**, (2020).
11. Rajendran, G. *et al.* Epigenetic regulation of DNA methyltransferases: DNMT1 and DNMT3B in gliomas. *J Neurooncol* **104**, 483–494 (2011).
12. Yang, Z. *et al.* 2-HG Inhibits Necroptosis by Stimulating DNMT1-Dependent Hypermethylation of the RIP3 Promoter. *Cell Rep* **19**, 1846–1857 (2017).
13. Turcan, S. *et al.* Efficient induction of differentiation and growth inhibition in IDH1 mutant glioma cells by the DNMT Inhibitor Decitabine. *Oncotarget* **4**, 1729–36 (2013).
14. Yamashita, A. S. *et al.* Demethylation and epigenetic modification with 5-azacytidine reduces IDH1 mutant glioma growth in combination with temozolomide. *Neuro Oncol* **21**, 189–200 (2019).

15. Turcan, S. *et al.* IDH1 mutation is sufficient to establish the glioma hypermethylator phenotype. *Nature* **483**, 479–83 (2012).

16. Lu, C. *et al.* IDH mutation impairs histone demethylation and results in a block to cell differentiation. *Nature* **483**, 474 (2012).

17. Gunn, K. *et al.* (R)-2-Hydroxyglutarate Inhibits KDM5 Histone Lysine Demethylases to Drive Transformation in IDH-Mutant Cancers. *Cancer Discov* **13**, 1478–1497 (2023).

18. Pekmezci, M. *et al.* Loss of H3K27 trimethylation by immunohistochemistry is frequent in oligodendroglioma, IDH-mutant and 1p/19q-codeleted, but is neither a sensitive nor a specific marker. *Acta Neuropathol* **139**, 597–600 (2020).

19. Doll, S., Urisman, A., Oses-Prieto, J. A., Arnott, D. & Burlingame, A. L. Quantitative Proteomics Reveals Fundamental Regulatory Differences in Oncogenic HRAS and Isocitrate Dehydrogenase (IDH1) Driven Astrocytoma. *Mol Cell Proteomics* **16**, 39–56 (2017).

20. Lucio-Eterovic, A. K. B. *et al.* Differential expression of 12 histone deacetylase (HDAC) genes in astrocytomas and normal brain tissue: class II and IV are hypoexpressed in glioblastomas. *BMC Cancer* **8**, 243 (2008).

21. Garrett, M. C. *et al.* HDAC1 and HDAC6 are essential for driving growth in IDH1 mutant glioma. (2022) doi:10.21203/rs.3.rs-1720726/v1.

22. Kim, G. H. *et al.* IDH1R132H Causes Resistance to HDAC Inhibitors by Increasing NANOG in Glioblastoma Cells. *Int J Mol Sci* **20**, (2019).

23. Chang, C. M. *et al.* Mutant Isocitrate Dehydrogenase 1 Expression Enhances Response of Gliomas to the Histone Deacetylase Inhibitor Belinostat. *Tomography* **9**, 942 (2023).

24. Kayabolen, A. & Cingoz, A. Combined inhibition of KDM6A/B and HDACs exacerbates integrated stress response and mediates therapeutic effects in IDH1-mutant glioma Basic Spine Surgery Educational DVD Series View project. doi:10.1101/2020.11.26.400234.

25. Sears, T. K., Horbinski, C. M. & Woolard, K. D. IDH1 mutant glioma is preferentially sensitive to the HDAC inhibitor panobinostat. *J Neurooncol* **154**, 159 (2021).

26. Turcan, S. *et al.* Mutant-IDH1-dependent chromatin state reprogramming, reversibility, and persistence. *Nature Genetics 2017 50:1* **50**, 62–72 (2017).

27. Al-Ali, R. *et al.* Single-nucleus chromatin accessibility reveals intratumoral epigenetic heterogeneity in IDH1 mutant gliomas. *Acta Neuropathol Commun* **7**, 201 (2019).

28. Garrett, M. C. *et al.* Chromatin structure predicts survival in glioma patients. *Sci Rep* **12**, 8221 (2022).

29. Gelman, S. J. *et al.* Consumption of NADPH for 2-HG Synthesis Increases Pentose Phosphate Pathway Flux and Sensitizes Cells to Oxidative Stress. *Cell Rep* **22**, 512 (2018).

30. Badur, M. G. *et al.* Oncogenic R132 IDH1 Mutations Limit NADPH for De Novo Lipogenesis through (D)2-Hydroxyglutarate Production in Fibrosarcoma Cells. *Cell Rep* **25**, 1018 (2018).

31. Bleeker, F. E. *et al.* The prognostic IDH1R132 mutation is associated with reduced NADP+-dependent IDH activity in glioblastoma. *Acta Neuropathol* **119**, 487 (2010).

32. Minami, J. K. *et al.* CDKN2A deletion remodels lipid metabolism to prime glioblastoma for ferroptosis. *Cancer Cell* **41**, 1048-1060.e9 (2023).

33. Lita, A. *et al.* IDH1 mutations induce organelle defects via dysregulated phospholipids. *Nature Communications 2021 12:1* **12**, 1–16 (2021).

34. Röhrig, F. & Schulze, A. The multifaceted roles of fatty acid synthesis in cancer. *Nat Rev Cancer* **16**, 732–749 (2016).

35. Ricklefs, F. L. *et al.* FASN Is a Biomarker Enriched in Malignant Glioma-Derived Extracellular Vesicles. *Int J Mol Sci* **21**, (2020).

36. Zhou, Y. *et al.* Inhibition of fatty acid synthase suppresses neovascularization via regulating the expression of VEGF-A in glioma. *J Cancer Res Clin Oncol* **142**, 2447–2459 (2016).

37. Yasumoto, Y. *et al.* Inhibition of fatty acid synthase decreases expression of stemness markers in glioma stem cells. *PLoS One* **11**, (2016).

38. Grube, S. *et al.* Overexpression of fatty acid synthase in human gliomas correlates with the WHO tumor grade and inhibition with Orlistat reduces cell viability and triggers apoptosis. doi:10.1007/s11060-014-1452-z.

39. Eyme, K. M. *et al.* Targeting de novo lipid synthesis induces lipotoxicity and impairs DNA damage repair in glioblastoma mouse models. *Sci Transl Med* **15**, (2023).

40. Hari, A. D., Vegi, N. G. & Das, U. N. Arachidonic and eicosapentaenoic acids induce oxidative stress to suppress proliferation of human glioma cells. *Arch Med Sci* **16**, 974–983 (2020).

41. Wang, F. *et al.* Docosahexaenoic Acid (DHA) Sensitizes Brain Tumor Cells to Etoposide-Induced Apoptosis. *Curr Mol Med* **11**, 503 (2011).

42. Söderberg, M., Edlund, C., Kristensson, K. & Dallner, G. Fatty acid composition of brain phospholipids in aging and in Alzheimer's disease. *Lipids* **26**, 421–425 (1991).

43. Cheng, M., Bhujwalla, Z. M. & Glunde, K. Targeting Phospholipid Metabolism in Cancer. *Front Oncol* **6**, 266 (2016).

44. Hvinden, I. C., Cadoux-Hudson, T., Schofield, C. J. & McCullagh, J. S. O. Metabolic adaptations in cancers expressing isocitrate dehydrogenase mutations. *Cell Rep Med* **2**, (2021).

45. Fack, F. *et al.* Altered metabolic landscape in IDH -mutant gliomas affects phospholipid, energy, and oxidative stress pathways . *EMBO Mol Med* **9**, 1681–1695 (2017).

46. Reitman, Z. J. *et al.* Profiling the effects of isocitrate dehydrogenase 1 and 2 mutations on the cellular metabolome. *Proc Natl Acad Sci U S A* **108**, 3270–3275 (2011).

47. Viswanath, P. *et al.* 2-Hydroxyglutarate-Mediated Autophagy of the Endoplasmic Reticulum Leads to an Unusual Downregulation of Phospholipid Biosynthesis in Mutant IDH1 Gliomas. *Cancer Res* **78**, 2290–2304 (2018).

48. Luo, J., Yang, H. & Song, B. L. Mechanisms and regulation of cholesterol homeostasis. *Nature Reviews Molecular Cell Biology 2019 21:4* **21**, 225–245 (2019).

49. Zhu, J. *et al.* Expression of R132H Mutational IDH1 in Human U87 Glioblastoma Cells Affects the SREBP1a Pathway and Induces Cellular Proliferation. *Journal of Molecular Neuroscience* **50**, 165–171 (2012).

50. Wang, T. *et al.* PERK-Mediated Cholesterol Excretion from IDH Mutant Glioma Determines Anti-Tumoral Polarization of Microglia. *Advanced Science* (2023) doi:10.1002/ADVS.202205949.

51. Yang, R. *et al.* Isocitrate dehydrogenase 1 mutation enhances 24(S)-hydroxycholesterol production and alters cholesterol homeostasis in glioma. *Oncogene 2020 39:40* **39**, 6340–6353 (2020).

52. Nie, Q. M. *et al.* IDH1R132H decreases the proliferation of U87 glioma cells through upregulation of microRNA-128a. *Mol Med Rep* **12**, 6695–6701 (2015).

53. Johannessen, T. C. A. *et al.* Rapid Conversion of Mutant IDH1 from Driver to Passenger in a Model of Human Gliomagenesis. *Mol Cancer Res* **14**, 976 (2016).

54. Haddad, A. F. *et al.* Mouse models of glioblastoma for the evaluation of novel therapeutic strategies. *Neurooncol Adv* **3**, 1–16 (2021).

55. Dow, J. *et al.* Vulnerability of IDH1 mutant cancers to histone deacetylase inhibition via orthogonal suppression of DNA repair. *Mol Cancer Res* **19**, 2057–2067 (2021).

56. Núñez, F. J. *et al.* IDH1-R132H acts as a tumor suppressor in glioma via epigenetic up-regulation of the DNA damage response. *Sci Transl Med* **11**, 1427 (2019).

57. Núñez, F. J. *et al.* IDH1-R132H acts as a tumor suppressor in glioma via epigenetic up-regulation of the DNA damage response. *Sci Transl Med* **11**, (2019).

58. Garrett, M. *et al.* Metabolic characterization of isocitrate dehydrogenase (IDH) mutant and IDH wildtype gliomaspheres uncovers cell type-specific vulnerabilities. *Cancer Metab* **6**, 4 (2018).

59. Shi, D. D. *et al.* De novo pyrimidine synthesis is a targetable vulnerability in IDH mutant glioma. *Cancer Cell* **40**, 939-956.e16 (2022).

60. Abdullah, K. G. *et al.* Establishment of patient-derived organoid models of lower-grade glioma. *Neuro Oncol* **24**, 612–623 (2022).

61. Laks, D. R. *et al.* Large-scale assessment of the gliomasphere model system. *Neuro Oncol* **18**, 1367 (2016).

62. Moure, C. J. *et al.* CRISPR editing of mutant IDH1 R132H induces a CpG methylation-low state in patient-derived glioma models of G-CIMP. *Mol Cancer Res* **17**, 2042 (2019).

63. Mazor, T. *et al.* Clonal expansion and epigenetic reprogramming following deletion or amplification of mutant IDH1. *Proc Natl Acad Sci U S A* **114**, 10743–10748 (2017).

64. Tateishi, K. *et al.* Extreme vulnerability of IDH1 mutant cancers to NAD+ depletion. *Elsevier*.

65. Turcan, S. *et al.* Mutant-IDH1-dependent chromatin state reprogramming, reversibility, and persistence. *Nat Genet* **50**, 62–72 (2018).

66. Pusch, S. *et al.* Pan-mutant IDH1 inhibitor BAY 1436032 for effective treatment of IDH1 mutant astrocytoma in vivo. *Acta Neuropathol* **133**, 629–644 (2017).

67. Rohle, D. *et al.* An inhibitor of mutant IDH1 delays growth and promotes differentiation of glioma cells. *Science* **340**, 626–630 (2013).

68. King, J., Patel, M. & Chandrasekaran, S. Metabolism, HDACs, and HDAC Inhibitors: A Systems Biology Perspective. *Metabolites* **11**, (2021).

69. Li, W. & Sun, Z. Mechanism of action for HDAC inhibitors—Insights from omics approaches. *Int J Mol Sci* **20**, (2019).

70. Ramaiah, M. J., Tangutur, A. D. & Manyam, R. R. Epigenetic modulation and understanding of HDAC inhibitors in cancer therapy. *Life Sci* **277**, 119504 (2021).

71. Lin, H. P. *et al.* Destabilization of fatty acid synthase by acetylation inhibits de novo lipogenesis and tumor cell growth. *Cancer Res* **76**, 6924 (2016).

72. Lu, X. *et al.* HOXB13 suppresses de novo lipogenesis through HDAC3-mediated epigenetic reprogramming in prostate cancer. *Nat Genet* **54**, 670–683 (2022).

73. Badur, M. G. *et al.* Oncogenic R132 IDH1 Mutations Limit NADPH for De Novo Lipogenesis through (D)2-Hydroxyglutarate Production in Fibrosarcoma Cells. *Cell Rep* **25**, 1018 (2018).

74. Gelman, S. J. *et al.* Consumption of NADPH for 2-HG Synthesis Increases Pentose Phosphate Pathway Flux and Sensitizes Cells to Oxidative Stress. *Cell Rep* **22**, 512–522 (2018).

75. Gurvich, N., Tsygankova, O. M., Meinkoth, J. L. & Klein, P. S. Histone Deacetylase Is a Target of Valproic Acid-Mediated Cellular Differentiation. *Cancer Res* **64**, 1079–1086 (2004).

76. Romoli, M. *et al.* Valproic Acid and Epilepsy: From Molecular Mechanisms to Clinical Evidences. *Curr Neuropharmacol* **17**, 926–946 (2019).

77. Benatti, P. *et al.* NF-Y activates genes of metabolic pathways altered in cancer cells. *Oncotarget* **7**, 1633 (2016).

78. Peterson, T. R. *et al.* MTOR complex 1 regulates lipin 1 localization to control the srebp pathway. *Cell* **146**, 408–420 (2011).

79. Raab, S. *et al.* Dual regulation of fatty acid synthase (FASN) expression by O-GlcNAc transferase (OGT) and mTOR pathway in proliferating liver cancer cells. *Cell Mol Life Sci* **78**, 5397–5413 (2021).

80. Han, J. & Kaufman, R. J. Thematic Review Series: Lipotoxicity: Many Roads to Cell Dysfunction and Cell Death: The role of ER stress in lipid metabolism and lipotoxicity. *J Lipid Res* **57**, 1329 (2016).

81. Yuan, Y., Shah, N., Almohaisin, M. I., Saha, S. & Lu, F. Assessing fatty acid-induced lipotoxicity and its therapeutic potential in glioblastoma using stimulated Raman microscopy. *Sci Rep* **11**, (2021).

82. Kim, S. *et al.* ω3-polyunsaturated fatty acids induce cell death through apoptosis and autophagy in glioblastoma cells: In vitro and in vivo. *Oncol Rep* **39**, 239–246 (2018).

83. Lita, A. *et al.* IDH1 mutations induce organelle defects via dysregulated phospholipids. *Nat Commun* **12**, (2021).

84. Nakajima, S., Gotoh, M., Fukasawa, K., Murakami-Murofushi, K. & Kunugi, H. Oleic acid is a potent inducer for lipid droplet accumulation through its esterification to glycerol by diacylglycerol acyltransferase in primary cortical astrocytes. *Brain Res* **1725**, (2019).

85. Lin, H. P. *et al.* Destabilization of fatty acid synthase by acetylation inhibits de novo lipogenesis and tumor cell growth. *Cancer Res* **76**, 6924 (2016).

86. Sperry, J. *et al.* Glioblastoma Utilizes Fatty Acids and Ketone Bodies for Growth Allowing Progression during Ketogenic Diet Therapy. *iScience* **23**, 101453 (2020).

87. Chang, C. M. *et al.* Mutant Isocitrate Dehydrogenase 1 Expression Enhances Response of Gliomas to the Histone Deacetylase Inhibitor Belinostat. *Tomography* **9**, 942–954 (2023).

88. RIVA, G. *et al.* Epigenetic targeting of glioma stem cells: Short-term and long-term treatments with valproic acid modulate DNA methylation and differentiation behavior, but not temozolomide sensitivity. *Oncol Rep* **35**, 2811–2824 (2016).

89. Lunke, S. *et al.* Epigenetic evidence of an Ac/Dc axis by VPA and SAHA. *Clin Epigenetics* **13**, (2021).

90. Xu, S. *et al.* Lipidomic Profiling Reveals Disruption of Lipid Metabolism in Valproic Acid-Induced Hepatotoxicity. *Front Pharmacol* **10**, (2019).

91. Płonka-Półtorak, E. *et al.* Does valproate therapy in epileptic patients contribute to changing atherosclerosis risk factors? The role of lipids and free fatty acids. *Pharmacological Reports* **68**, 1339–1344 (2016).

92. Grünig, D., Szabo, L., Marbet, M. & Krähenbühl, S. Valproic acid affects fatty acid and triglyceride metabolism in HepaRG cells exposed to fatty acids by different mechanisms. *Biochem Pharmacol* **177**, (2020).

93. Zhao, S. *et al.* Regulation of Cellular Metabolism by Protein Lysine Acetylation. *Science* **327**, 1000 (2010).

94. Wang, Q. *et al.* Acetylation of Metabolic Enzymes Coordinates Carbon Source Utilization and Metabolic Flux. *Science* **327**, 1004 (2010).

95. Ocker, M. Deacetylase inhibitors - focus on non-histone targets and effects. *World J Biol Chem* **1**, 55 (2010).

96. Sun, Z. *et al.* Hepatic Hdac3 promotes gluconeogenesis by repressing lipid synthesis and sequestration. *Nat Med* **18**, 934 (2012).

97. Peng, Y. *et al.* Irradiation modulates association of NF-Y with histone-modifying cofactors PCAF and HDAC. *Oncogene 2007 26:54* **26**, 7576–7583 (2007).

98. Fu, X. *et al.* 2-Hydroxyglutarate Inhibits ATP Synthase and mTOR Signaling. *Cell Metab* **22**, 508–515 (2015).

99. Carbonneau, M. *et al.* The oncometabolite 2-hydroxyglutarate activates the mTOR signalling pathway. *Nat commun* **7**, 12700 (2016).

100. Batsios, G. *et al.* PI3K/mTOR inhibition of IDH1 mutant glioma leads to reduced 2HG production that is associated with increased survival. *Sci Rep* **9**, (2019).

101. Mohamed, E. *et al.* PI3K/AKT/mTOR signaling pathway activity in IDH-mutant diffuse glioma and clinical implications. *Neuro Oncol* **24**, 1471–1481 (2022).

102. Zhang, X. *et al.* PI3K/AKT/mTOR Signaling Mediates Valproic Acid-Induced Neuronal Differentiation of Neural Stem Cells through Epigenetic Modifications. *Stem Cell Reports* **8**, 1256–1269 (2017).

103. Han, W. *et al.* Valproic Acid Enhanced Apoptosis by Promoting Autophagy Via Akt/mTOR Signaling in Glioma. *Cell Transplant* **29**, (2020).

104. Sun, J. *et al.* Valproic acid targets HDAC1/2 and HDAC1/PTEN/Akt signalling to inhibit cell proliferation via the induction of autophagy in gastric cancer. *FEBS Journal* **287**, 2118–2133 (2020).

105. Xia, Q. *et al.* Valproic acid induces autophagy by suppressing the Akt/mTOR pathway in human prostate cancer cells. *Oncol Lett* **12**, 1826–1832 (2016).

106. Harachi, M. *et al.* mTOR Complexes as a Nutrient Sensor for Driving Cancer Progression. *Int J Mol Sci* **19**, (2018).

107. Menon, D. *et al.* Lipid sensing by mTOR complexes via de novo synthesis of phosphatidic acid. *J Biol Chem* **292**, 6303 (2017).

108. Xie, Q. B. *et al.* DEPTOR-mTOR Signaling Is Critical for Lipid Metabolism and Inflammation Homeostasis of Lymphocytes in Human PBMC Culture. *J Immunol Res* **2017**, (2017).

109. Daemen, A. *et al.* Metabolite profiling stratifies pancreatic ductal adenocarcinomas into subtypes with distinct sensitivities to metabolic inhibitors. *Proc Natl Acad Sci U S A* **112**, E4410–E4417 (2015).

110. Ahler, E. *et al.* Doxycycline Alters Metabolism and Proliferation of Human Cell Lines. *PLoS One* **8**, 64561 (2013).

111. Alwarawrah, Y. *et al.* Fasnall, a Selective FASN Inhibitor, Shows Potent Anti-tumor Activity in the MMTV-Neu Model of HER2(+) Breast Cancer. *Cell Chem Biol* **23**, 678–688 (2016).

112. Oh, J. E., Jung, B. H., Park, J., Kang, S. & Lee, H. Deciphering Fatty Acid Synthase Inhibition-Triggered Metabolic Flexibility in Prostate Cancer Cells through Untargeted Metabolomics. *Cells* **9**, (2020).

113. Fader Kaiser, C. M. *et al.* Biogenesis and Breakdown of Lipid Droplets in Pathological Conditions. *Front Cell Dev Biol* **9**, (2022).

114. Harris, C. A. *et al.* DGAT enzymes are required for triacylglycerol synthesis and lipid droplets in adipocytes. *J Lipid Res* **52**, 657–667 (2011).

115. Lu, X. *et al.* HOXB13 suppresses de novo lipogenesis through HDAC3-mediated epigenetic reprogramming in prostate cancer. *Nature Genetics 2022 54:5* **54**, 670–683 (2022).

116. Núñez, F. J. *et al.* IDH1-R132H acts as a tumor suppressor in glioma via epigenetic up-regulation of the DNA damage response. *Sci Transl Med* **11**, (2019).

117. Corces, M. R. *et al.* An improved ATAC-seq protocol reduces background and enables interrogation of frozen tissues. *Nat Methods* **14**, 959 (2017).

118. Kelly, W. *et al.* Phase II Investigation of TVB-2640 (Denifanstat) with Bevacizumab in Patients with First Relapse High-Grade Astrocytoma. *Clin Cancer Res* **29**, OF1–OF7 (2023).